Molecular Pharmacology Fast Forward. Published on June 13, 2016 as DOI: 10.1124/mol.116.103648
This article has not been copyedited and formatted. The final version may differ from this version.

Arsenic Triglutathione [$As(GS)_3$] Transport by Multidrug Resistance Protein 1 (MRP1/*ABCC1*) is Selectively Modified by Phosphorylation of Tyr920/Ser921 and Glycosylation of Asn19/Asn23.

Caley B. Shukalek, Diane P. Swanlund, Rodney K. Rousseau, Kevin E. Weigl, Vanessa Marensi, Susan P.C. Cole, and Elaine M. Leslie

Department of Physiology *(CBS, DPS, RKR, VM, EML)* and Membrane Protein Disease Research Group *(CBS, DPS, RKR, VM, EML)*, University of Alberta, Edmonton, Alberta, Canada. Department of Pathology and Molecular Medicine and Division of Cancer Biology and Genetics *(KEW, SPCC)*, Queen's University, Kingston, Ontario, Canada

Molecular Pharmacology Fast Forward. Published on June 13, 2016 as DOI: 10.1124/mol.116.103648
This article has not been copyedited and formatted. The final version may differ from this version.

Running Title: Phosphorylation & Glycosylation Selectively Modify MRP1 Function

Corresponding author: Elaine M. Leslie, Department of Physiology, 7-08A Medical Sciences Building, University of Alberta, Edmonton, AB, Canada, Tel.: (780) 492 9250; Fax: (780) 248 1995; email: eleslie@ualberta.ca.

Text pages: 27

Tables: 2

Figures: 7

References: 67

Abstract: 250 words

Introduction: 766 words

Discussion: 1557

Supplemental Tables: 2

Supplemental Figures: 2

Non-standard abbreviations: ABC, ATP-binding cassette; As^{V}, arsenate; As^{III}, arsenite; $As(GS)_3$, arsenic triglutathione; CIP, Calf Intestinal Alkaline Phosphatase; CL3, cytoplasmic loop 3; DMA^{III}, dimethylarsinous acid; DMA^{V}, dimethylarsinic acid; $E_2$17βG, 17β-estradiol 17-(β-D-glucuronide); GLUT1, glucose transporter 1; LTC_4, leukotriene C_4; mAb, monoclonal antibody; MMA^{III}, monomethylarsonous acid; MMA^{V}, monomethylarsonic acid; $MMA(GS)_2$, monomethylarsenic diglutathione; MRP, multidrug resistance protein; MSD, membrane spanning domain; NBD, nucleotide binding domain; pAb, polyclonal antibody; PIC, phosphatase inhibitor cocktail; PNGase F, Peptide: N-glycosidase F; PTP, protein tyrosine phosphatase; SF, sugar free; TM, transmembrane helix; TPCK, L-1-tosylamido-2-phenylethyl chloromethyl ketone

Molecular Pharmacology Fast Forward. Published on June 13, 2016 as DOI: 10.1124/mol.116.103648
This article has not been copyedited and formatted. The final version may differ from this version.

ABSTRACT

The ATP-binding cassette (ABC) transporter MRP1 (*ABCC1*) is responsible for the cellular export of a chemically diverse array of xenobiotics and endogenous compounds. Arsenic, a human carcinogen, is a high affinity MRP1 substrate as arsenic triglutathione [$As(GS)_3$]. In this study, marked differences in $As(GS)_3$ transport kinetics were observed between MRP1-enriched membrane vesicles prepared from HEK293 (K_m 3.8 μM and V_{max} 307 pmol/mg/min) and HeLa (K_m 0.32 μM and V_{max} 42 pmol/mg/min) cells. Mutant MRP1 lacking *N*-linked glycosylation [Asn19/23/1006Gln; sugar-free (SF)-MRP1] expressed in either HEK293 or HeLa cells had low K_m and V_{max} values for $As(GS)_3$, similar to HeLa-WT-MRP1. When prepared in the presence of phosphatase inhibitors, both WT- and SF-MRP1-enriched membrane vesicles had a high K_m for $As(GS)_3$ (3-6 μM), regardless of the cell line. Kinetic parameters of $As(GS)_3$ for HEK-Asn19/23Gln-MRP1 were similar to HeLa/HEK-SF-MRP1 and HeLa-WT-MRP1, while those of single glycosylation mutants were like HEK-WT-MRP1. Mutation of 19 potential MRP1 phosphorylation sites revealed that HEK-Tyr920Phe/Ser921Ala-MRP1 transported $As(GS)_3$ like HeLa-WT-MRP1, while individual HEK-Tyr920Phe and -Ser921Ala mutants were similar to HEK-WT-MRP1. Together these results suggest that Asn19/Asn23 glycosylation and Tyr920/Ser921 phosphorylation are responsible for altering the kinetics of MRP1-mediated $As(GS)_3$ transport. The kinetics of $As(GS)_3$ transport by HEK-Asn19/23Gln/Tyr920Glu/ Ser921Glu were similar to HEK-WT-MRP1 indicating that the phosphorylation-mimicking substitutions abrogated the influence of Asn19/23Gln glycosylation. Overall these data suggest that cross-talk between MRP1 glycosylation and phosphorylation occurs, and that phosphorylation of Tyr920 and Ser921 can switch MRP1 to a lower affinity, higher capacity $As(GS)_3$ transporter, allowing arsenic detoxification over a broad concentration range.

Molecular Pharmacology Fast Forward. Published on June 13, 2016 as DOI: 10.1124/mol.116.103648
This article has not been copyedited and formatted. The final version may differ from this version.

INTRODUCTION

Arsenic, a group 1 (proven) human carcinogen, is an element found throughout the earth's crust resulting in human exposure through groundwater (Garelick et al., 2008). Chronic exposure to arsenic is known to cause cancers of the lung, skin and bladder and is associated with increased incidences of liver and kidney tumors (IARC, 2012). In addition to cancer, arsenic exposure is associated with other adverse health effects such as diabetes and hypertension (Platanias, 2009). Somewhat paradoxically, arsenic trioxide (As_2O_3) is highly effective in the treatment of acute promyelocytic leukemia and more recently is in clinical trials as a therapy for other hematological and solid tumors (Kritharis et al., 2013).

The structural resemblance of arsenate (As^V) to phosphate allows its cellular uptake through phosphate carriers such as the Na^+/phosphate co-transporter type IIb (*SLC34A2*) (Villa-Bellosta and Sorribas, 2010). In aqueous solution at physiological pH, arsenite (As^{III}) and As_2O_3 exist as the neutral $As(OH)_3$ and can enter cells passively through aquaglyceroporin channels as well as the glucose transporter 1 (GLUT1/*SLC2A1*) (Mukhopadhyay et al., 2014; Ramirez-Solis et al., 2004).Once inside human cells, arsenic can be methylated to four major products: monomethylarsonic acid (MMA^V), monomethylarsonous acid (MMA^{III}), dimethylarsinic acid (DMA^V), and dimethylarsinous acid (DMA^{III}) (Drobna et al., 2010). While arsenic methylation increases its whole body clearance, it is considered a bioactivation pathway because MMA^{III} and DMA^{III} are more toxic than inorganic arsenic (Mass et al., 2001; Petrick et al., 2000). Arsenic also undergoes conjugation with GSH (Leslie, 2012). Thus, As^{III} and MMA^{III} as $As(GS)_3$ and $MMA(GS)_2$, respectively, have been isolated from rodent bile and urine (Kala et al., 2004; Kala et al., 2000).

Molecular Pharmacology Fast Forward. Published on June 13, 2016 as DOI: 10.1124/mol.116.103648
This article has not been copyedited and formatted. The final version may differ from this version.

Inorganic, methylated and glutathionylated arsenic species can be actively removed from the cell through ATP-dependent transport proteins while neutral species can be passively extruded through the aquaglyceroporins (Leslie, 2012; Mukhopadhyay et al., 2014). The multidrug resistance proteins MRP1, MRP2, and MRP4 (gene symbols *ABCC1*, *ABCC2*, and *ABCC4*, respectively) are ATP-binding cassette (ABC) transporter proteins with established roles as arsenic efflux pumps (Banerjee et al., 2014; Carew and Leslie, 2010; Kala et al., 2000; Leslie et al., 2004).

The 190 kDa phosphoglycoprotein MRP1 was originally identified based on its ability to confer resistance to a structurally diverse array of anti-cancer agents through an ATP-dependent decrease in cellular drug accumulation (Cole, 2013). In addition to its role in drug resistance, MRP1 is important for the transport of physiological substrates including mediators of inflammation such as leukotriene C_4 (LTC_4) and the cholestatic steroid 17β-estradiol 17-(β-D-glucuronide) ($E_2$17βG) (Cole, 2014). Furthermore, MRP1 transports a variety of other drugs, toxicants, and carcinogens often conjugated to GSH, glucuronate, or sulphate (Jedlitschky et al., 1996; Leslie et al., 2005; Loe et al., 1996a; Loe et al., 1996b). $As(GS)_3$ was first identified, using membrane vesicles isolated from the doxorubicin-selected human small cell lung cancer cell line H69AR, as a high affinity low capacity substrate of MRP1 with a K_m of 0.32 μM and V_{max} of 17 pmol mg^{-1} min^{-1} (Leslie et al., 2004).

Despite the numerous and important physiological, pharmacological, and toxicological roles MRP1 plays, the influence of post-translational modifications on its functional regulation are not well characterized. MRP1 has three utilized *N*-glycosylation sites at Asn19, Asn23 [in the first membrane spanning domain (MSD0)] and Asn1006 [in the first extracellular loop of MSD2 connecting transmembrane helix (TM) 12 to TM13] (Hipfner et al., 1997) and is known to be

Molecular Pharmacology Fast Forward. Published on June 13, 2016 as DOI: 10.1124/mol.116.103648
This article has not been copyedited and formatted. The final version may differ from this version.

phosphorylated (Almquist et al., 1995; Ma et al., 1995). Although mass spectrometry-based proteomic studies have identified 20 phosphorylation sites on MRP1 to date (Hornbeck et al., 2015), only one site (Thr249) in cytoplasmic loop 3 (CL3) which connects TM5 to TM6 has been functionally characterized (Stolarczyk et al., 2012).

In the current study, MRP1 expressed in HeLa cells was shown to have a 12-fold lower K_m and 7-fold lower V_{max} for $As(GS)_3$ than observed for MRP1 expressed in HEK293 cells. Our findings indicate that MRP1 is differentially *N*-glycosylated and phosphorylated in membrane vesicles prepared from the two cell lines. We also found that the affinity and capacity of MRP1 for $As(GS)_3$ can be modulated by dual glycosylation at Asn19 and Asn23 as well as dual phosphorylation of MRP1 at Tyr920 and Ser921. Evidence is presented that the phosphorylation of Tyr920/Ser921 results in the markedly lower affinity and higher capacity of $As(GS)_3$ transport by MRP1. In addition, the glycosylation status of Asn19/Asn23 influenced the phosphorylation at Tyr920/Ser921, suggesting cross-talk between these two post-translational modifications. Together, our findings suggest that the affinity of MRP1 for $As(GS)_3$ is influenced by cell type, phosphorylation, and glycosylation which has important implications for arsenic detoxification by different cell types and tissues over a broad concentration range of this carcinogen.

Molecular Pharmacology Fast Forward. Published on June 13, 2016 as DOI: 10.1124/mol.116.103648
This article has not been copyedited and formatted. The final version may differ from this version.

MATERIALS AND METHODS

Materials. Carrier-free $^{73}As^{V}$ (158 Ci/mol) was purchased from Los Alamos Meson Production Facility (Los Alamos, NM) and carrier-free [6', 7'-^{3}H]$E_2$17βG (30-60 Ci/mmol) was obtained from PerkinElmer Life and Analytical Sciences (Woodbridge, ON). [3', 5', 7-^{3}H(N)]-methotrexate (13.4 Ci/mmol) was purchased from Moravek Biochemicals Inc. (Brea, CA). Creatine kinase (rabbit muscle), creatine phosphate, GSH reductase (yeast), Complete™ mini EDTA-free and EDTA-containing protease inhibitor cocktail tablets, and PhosSTOP™ phosphatase inhibitor cocktail (PIC) tablets were purchased from Roche Applied Science (Laval, QC). Calf intestinal alkaline phosphatase (CIP) was purchased from New England Biolabs Canada (Whitby, ON). Sodium (meta)-arsenite [Na_2AsO_2], sodium metabisulfite [$Na_2S_2O_5$], sodium thiosulfate [$Na_2S_2O_3$], $E_2$17βG, bovine serum albumin (BSA), and GSH were obtained from Sigma-Aldrich (Oakville, ON). L-1-Tosylamido-2-phenylethyl chloromethyl ketone (TPCK)-treated trypsin was purchased from Thermo Scientific (Rockford, IL). PMSF was from Bioshop Canada Inc. (Burlington, ON). Sodium orthovanadate was from Tocris Bioscience (Bristol, UK). MRP1-specific antibodies used in this study include: the rat monoclonal antibody (mAb) MRPr1 from Novus Biologicals (Littleton, CO), and the mouse mAb MRPm6 from Millipore (Temecula, CA). The mouse mAb QCRL1 and rabbit polyclonal antibody (pAb) MRP-1 were produced as described (Hipfner et al., 1996; Hipfner et al., 1994). Rabbit anti-Na^+/K^+ATPase (H-300) was purchased from Santa Cruz Biotechnology, Inc. (Santa Cruz, CA).

Cell lines and stable transfection. HEK293 cells were obtained from the American Type Culture Collection (Rockville, MD) and maintained in Dulbecco's modified Eagle's medium (DMEM) with 7.5% fetal bovine serum (FBS). HeLa cell lines stably expressing the empty pcDNA3.1(-) vector, pcDNA3.1(-)-MRP1 (HeLa-MRP1), or pcDNA3.1(-)-sugar-free (SF)-

Molecular Pharmacology Fast Forward. Published on June 13, 2016 as DOI: 10.1124/mol.116.103648
This article has not been copyedited and formatted. The final version may differ from this version.

MRP1 (HeLa-SF-MRP1) were generated as described previously (Ito et al., 2001; Weigl, 2005) and maintained in Roswell Park Memorial Institute (RPMI)-1640 medium with 5% calf serum and 600 μg/ml Geneticin (G418).

Site-directed mutagenesis. Mutants of MRP1 were generated using the Agilent QuikChange Lightning site-directed mutagenesis kit (Mississauga, ON). Mutagenesis was performed using pcDNA3.1(-)-MRP1 (Ito et al., 2001) as the PCR template (unless otherwise noted) according to the manufacturer's instructions. Mutagenic primers [Sigma-Aldrich (Oakville, ON) or Integrated DNA Technology (Coralville, IA)] were designed to mutate Asn residues shown previously to undergo glycosylation to Gln (Hipfner et al., 1997) as well as potential phosphorylation sites (Supplemental Table 1). Specifically, eight potential phosphorylation sites in CL3 were mutated individually from Ser, Thr or Tyr to Ala. In addition, a single construct with all eight potential phosphorylation sites mutated to Ala (Thr249Ala/ Ser250Ala/Thr268Ala/Tyr277Ala/Ser278Ala/Ser279Ala/Ser288Ala /Ser289Ala/ Ser289Ala) was generated and named 8X_CL3. 8X_CL3 was made using the pcDNA3.1-MRP1-Ser279Ala template with the Thr268Ala primer followed by the following primers: Thr249Ala/Ser250Ala, Tyr277Phe/Ser278Ala/Ser 279Ala, and Ser288Ala/Ser289Ala (Supplemental Table 1). Eleven potential phosphorylation sites in the linker region between NBD1 and MSD2 were mutated from Ser or Thr to Ala and Tyr to Phe. Tyr920 and Ser921 were also mutated to the phosphorylation mimicking Glu.

All mutants were confirmed by sequencing (MacrogenUSA, Rockville, MD or The Hospital for Sick Children, Toronto, ON). For mutants that exhibited transport activity different than WT-MRP1, the entire cDNA was sequenced to confirm that only the desired mutation had been introduced.

Molecular Pharmacology Fast Forward. Published on June 13, 2016 as DOI: 10.1124/mol.116.103648
This article has not been copyedited and formatted. The final version may differ from this version.

Transient expression of WT and mutant forms of MRP1 in HEK293 cells. HEK293 cells were transiently transfected with WT and mutant pcDNA3.1(-)-MRP1 vectors using a modified version of the calcium-phosphate transfection method (Chen and Okayama, 1988). Briefly, $3x10^6$ cells were seeded in 15 cm plates, and 24 h later, 18 µg DNA was added using 2 ml of calcium-phosphate transfection solution (125 mM $CaCl_2$, 140 mM NaCl, 0.75 mM $NaHPO_4$, 28 mM HEPES [pH 7.0]. The media was changed after 24 h, and cells were harvested at 72 h. Harvested cells were layered with Tris-sucrose buffer (50 mM Tris, pH 7.4, 250 mM sucrose) containing $CaCl_2$ (0.25 mM), EDTA-free protease inhibitors, and where indicated, phosSTOP PIC and stored at -80°C.

Membrane vesicle preparation and immunoblotting. Membrane vesicles were prepared using the nitrogen cavitation method as previously described (Carew and Leslie, 2010). Membrane vesicle proteins were resolved on SDS-PAGE gels (Hipfner et al., 1997) and transferred to a PVDF membrane and immunoblotted in 4% skim milk to determine relative expression levels using the MRP1-specific Abs: MRPr1 (diluted 1:10,000), QCRL1 (diluted 1:10,000), MRP-1 (diluted 1:5,000), and/or MRPm6 (diluted 1:10,000). The Na^+/K^+ATPase (H-300) (diluted 1:1,000) specific antibody was used as a loading control. Relative levels of MRP1 were quantified using ImageJ software (National Institutes of Health, USA).

As(GS)$_3$ and [^{73}As](GS)$_3$] synthesis. Arsenite [$^{73}As^{III}$] was reduced from arsenate [$^{73}As^{V}$] as previously described (Reay and Asher, 1977). Briefly, $NaAsO_2$ (6 mM) was added to a metabisulfite-thiosulfate reagent (66 mM $Na_2S_2O_5$, 27 mM $Na_2S_2O_3$ and 82 mM H_2SO_4) and then serially diluted using arsenic-free metabisulfite-thiosulfate reagent. These were then added at a 1:1 ratio with carrier-free $^{73}As^{V}$ to form $^{73}As^{III}$, and incubated for a minimum of 12 h at room temperature. To form $As(GS)_3$ and $^{73}As(GS)_3$ the reagent mixture was then mixed at a 1:1 ratio

Molecular Pharmacology Fast Forward. Published on June 13, 2016 as DOI: 10.1124/mol.116.103648
This article has not been copyedited and formatted. The final version may differ from this version.

with reduced GSH (150 mM) and incubated for at least 30 min at room temperature to obtain the appropriate $As(GS)_3$ concentrations with a GSH concentration of 75 mM.

$As(GS)_3$ transport studies. $As(GS)_3$ transport assays were performed as previously described with minor modifications (Leslie et al., 2004). Briefly, 20 µg of membrane vesicles were incubated with $As(GS)_3$ (0.05 – 30 µM, 30 – 120 nCi), GSH reductase (0.6 U/ml), NADPH (0.35 mM), GSH (3 mM), AMP or ATP (4 mM), $MgCl_2$ (10 mM), creatine phosphate (10 mM), and creatine kinase (100 µg/ml) at 37°C for 60 s. Transport was then stopped by diluting with 800 µl of ice-cold Tris-sucrose buffer and filtered through glass fibre filters (type GF/B) using a 96-well plate Cell-Harvester (Perkin Elmer, Waltham, MA), washed five times with Tris-sucrose buffer, and radioactivity quantified by liquid scintillation counting. Data were plotted using Prism 5 (Graphpad Software, La Jolla, CA) and K_m and V_{max} values determined using Michaelis-Menten analysis.

$E_2$17βG and methotrexate transport studies. $E_2$17βG transport assays were performed essentially as described (Carew et al., 2011). Briefly, 5 µg of membrane vesicles were incubated with $E_2$17βG (0.1 – 30 µM, 40 – 80 nCi), AMP or ATP (4 mM), $MgCl_2$ (10 mM), creatine phosphate (10 mM), and creatine kinase (100 µg/ml) at 37°C for 90 s. Transport was then stopped and samples were processed and analyzed as described above for $As(GS)_3$.

[^{3}H]Methotrexate transport assays were performed by incubating membrane vesicles (10 µg protein) with methotrexate (100 µM, 250 nCi) and components described for $E_2$17βG at 37ºC for 20 min.

Glycolytic and proteolytic analysis of MRP1. Membrane vesicles were diluted to 2 µg/µl in 50 mM Tris buffer (pH 7.4) and subjected to limited trypsinolysis of MRP1 as previously described, with slight modifications (Hipfner et al., 1997). Briefly, MRP1-enriched

Molecular Pharmacology Fast Forward. Published on June 13, 2016 as DOI: 10.1124/mol.116.103648
This article has not been copyedited and formatted. The final version may differ from this version.

vesicles were incubated with TPCK-treated trypsin at a trypsin:membrane protein ratio of 1:500 (w:w) for 30 min at 37°C. Proteolysis was stopped by the addition of PMSF. Removal of total and core *N*-glycosylation by Peptide: N-glycosidase F (PNGase F) and Endoglycosidase H (Endo H) (New England Biolabs, Pickering, ON), respectively, from the diluted membrane vesicles was performed as previously described (Hipfner et al., 1997). Subsequent immunoblotting was performed as described above.

Immunoreactivity of HeLa- MRP1and HEK-MRP1 with mAb QCRL-1. SDS-PAGE and immunoblotting were done as described above, with the following exceptions. Where indicated, samples were prepared in Laemmli buffer containing PIC and immunoblotting was done in 4% BSA with 100 µM sodium orthovanadate. Blots were then stripped and treated with calf intestinal alkaline phosphatase (CIP, 20 U ml^{-1}) for 30 min at 37°C, then reprobed for MRP1 with QCRL-1. For comparison of HeLa-MRP1 with HEK-MRP1 levels, equal loading was confirmed with amido black staining of the blots instead of the Na^+/K^+-ATPase, which had different levels between the cell lines.

Molecular Pharmacology Fast Forward. Published on June 13, 2016 as DOI: 10.1124/mol.116.103648
This article has not been copyedited and formatted. The final version may differ from this version.

RESULTS

Kinetic analysis of $As(GS)_3$ transport by WT-MRP1 expressed in HeLa and HEK293 cells. During a study of MRP1 mutants transiently expressed in HEK293 cells, we observed a 12-fold difference in K_m value for WT MRP1-mediated $As(GS)_3$ vesicular transport compared to previously published data (Leslie et al., 2004; Shukalek and Leslie, 2011). To investigate this observation further, kinetic parameters were determined for $As(GS)_3$ transport by MRP1-enriched vesicles prepared from HeLa-WT-MRP1 and HEK-WT-MRP1 cells (Figure 1A and B and Table 1). For HeLa-WT-MRP1 vesicles, the K_m for $As(GS)_3$ was 0.32 ± 0.03 μM (Figure 1A and Table 1), consistent with the previously published value, 0.32 ± 0.08 μM, determined using H69AR human lung cancer cell membrane vesicles (Leslie et al., 2004). In contrast, the K_m value for $As(GS)_3$ transport determined using HEK-WT-MRP1 vesicles was 3.8 ± 1.2 μM (Figure 1B and Table 2). The capacity of $As(GS)_3$ transport by WT-MRP1 was also significantly different between the HeLa and HEK293 membrane vesicles, with a 7-fold higher V_{max} for HEK-WT-MRP1 versus HeLa-WT-MRP1 (42 ± 17 pmol/mg/min versus 307 ± 118 pmol/mg/min, respectively) after normalization for MRP1 protein levels (Figure 1A and B, Table 1, and Supplemental Table 2).

Kinetic analysis of $E_2$17βG transport by WT-MRP1 expressed in HeLa and HEK293 cells. The large difference between K_m values for $As(GS)_3$ transport between HEK- and HeLa-WT-MRP1 cell lines was not expected because this cell line difference had not been observed for other MRP1 substrates (Loe et al., 1996a; Loe et al., 1996b; Stride et al., 1997). For example, the K_m value of 105 ± 31 nM for LTC_4 determined using membrane vesicles prepared from WT-MRP1 transfected HeLa (T14) cells was very similar to the K_m of 98 nM determined using WT-MRP1 transfected HEK293 cells (Loe et al., 1996b). Furthermore, the K_m values for $E_2$17βG

Molecular Pharmacology Fast Forward. Published on June 13, 2016 as DOI: 10.1124/mol.116.103648
This article has not been copyedited and formatted. The final version may differ from this version.

determined using membrane vesicles from the same cell lines were almost identical (2.5 μM in HeLa and 2.9 μM in HEK293) (Loe et al., 1996a; Stride et al., 1997). Consistent with the published data, the K_m value of $E_2$17βG for HeLa-WT-MRP1 in the present study was 4.0 ± 2.6 μM and for HEK-WT-MRP1 was 2.5 ± 0.8 μM, values that are not significantly different from each other (Figure 1C and D). These data suggested that a difference in MRP1 exists between the two cell lines that influences the affinity of $As(GS)_3$ for MRP1, but not $E_2$17βG or LTC_4.

Molecular weight difference between MRP1 expressed in HeLa and HEK293 cells. To investigate the differences between WT-MRP1 expressed in HeLa versus HEK293 cells, the respective relative electrophoretic mobility was determined using SDS-PAGE followed by immunoblot analysis. Consistent with previous results we observed that WT-MRP1 expressed in HeLa cells migrated at ~190-kDa while HEK-WT-MRP1 migrated at ~180-kDa (lanes 5 and 1, respectively, Figure 2) (Stride et al., 1997). To determine if this shift in molecular weight was due to glycosylation, MRP1-enriched vesicles prepared from HEK293 and HeLa cells were treated with different glycosidase enzymes (Figure 2). Digestion with Endo H caused no shifts in MRP1 mobility, indicating that MRP1 within the plasma membrane-enriched vesicles was modified by complex glycosylation. On the other hand, complete removal of *N*-linked glycosylation using PNGase F resulted in the shift of HEK-WT-MRP1 and HeLa-WT-MRP1 to comparable mobilities of ~170 kDa. PNGase F treated WT-MRP1 had the same mobility as the SF-MRP1 (the Asn19/23/1006Gln-MRP1 mutant that lacks glycosylation) expressed in HeLa and HEK293 cells. Thus, HeLa- and HEK-WT-MRP1 were fully glycosylated; however, differential glycosylation was responsible for the lower molecular weight of HEK-WT-MRP1 compared with HeLa-WT-MRP1.

Molecular Pharmacology Fast Forward. Published on June 13, 2016 as DOI: 10.1124/mol.116.103648
This article has not been copyedited and formatted. The final version may differ from this version.

To determine if phosphorylation could also contribute to differences in the molecular weights of HEK-WT-MRP1 and HeLa-WT-MRP1, MRP1-enriched membrane vesicles were dephosphorylated by treatment with calf intestinal phosphatase. No shift in the molecular weight of either WT-MRP1 was detected (data not shown). However, the molecular weight of MRP1 (190 kDa) is very large relative to the molecular weight of a phosphate group (95 Da), making it difficult to draw conclusions from this observation.

Kinetic parameters of As(GS)$_3$ transport by SF-MRP1 expressed in HeLa and HEK293 cells. After establishing that the difference in molecular weight between WT-MRP1 expressed in HeLa versus HEK293 cells was associated with differential *N*-glycosylation, the functional relevance of this finding was investigated. Consequently, K_m and V_{max} values were determined for As(GS)$_3$ transport using HeLa- and HEK-SF-MRP1-enriched membrane vesicles. Unexpectedly, HeLa-SF-MRP1 and HEK-SF-MRP1 displayed similar high affinity (K_m 0.3 ± 0.1 µM and 0.6 ± 0.4 µM, respectively) and low capacity (V_{max} 44 ± 15 pmol/mg/min and 38 ± 21 pmol/mg/min, respectively) kinetic parameters, similar to those of HeLa-WT-MRP1 (Figure 3A and 3B and Table 1). This indicated that *N*-glycosylation influenced transport of As(GS)$_3$ by MRP1.

Kinetic analysis of $E_2$17βG transport by SF-MRP1 expressed in HeLa and HEK293 cells. Previous work on SF-MRP1 expressed in HeLa cells showed an increase in capacity of LTC_4 transport relative to HeLa-WT-MRP1, but no change in affinity (K_m) (Weigl, 2005). To determine if the shift in affinity observed for SF-MRP1 expressed in HEK293 cells occurs for other substrates, the kinetic parameters of $E_2$17βG transport by SF-MRP1 expressed in HeLa and HEK293 cells were determined. Consistent with the above-mentioned values for HeLa-WT-MRP1 and HEK-WT-MRP1 and the published data, the K_m value of $E_2$17βG transport for HeLa-

Molecular Pharmacology Fast Forward. Published on June 13, 2016 as DOI: 10.1124/mol.116.103648
This article has not been copyedited and formatted. The final version may differ from this version.

SF-MRP1 was 4.3 μM and HEK-SF-MRP1 was 5.9 μM (Figure 3C and 3D). These data suggest that although differential glycosylation of WT-MRP1 expressed in HEK293 versus HeLa cells is responsible for the shift in $As(GS)_3$ transport kinetic parameters, it does not influence the affinity of MRP1 for $E_2$17βG.

Kinetic analysis of $As(GS)_3$ transport by glycosylation mutants of MRP1 expressed in HEK293 cells. Due to the changes in $As(GS)_3$ kinetic parameters observed for SF-MRP1, the influence of glycosylation was further investigated. Single Asn19Gln, Asn23Gln, Asn1006Gln and double Asn19/23Gln mutants of MRP1 were generated, expressed in HEK293 cells, and membrane vesicles prepared and immunoblotted. A modest reduction in molecular weight for each single mutant and a more pronounced shift for the double Asn19/23Gln mutant was observed, indicating that all of the *N*-glycosylation sites were utilized in HEK293 cells (Figure 4A). Characterization of $As(GS)_3$ transport revealed that the kinetic parameters for the single glycosylation mutants were similar to HEK-WT-MRP1 with high K_m (range 3 to 5 μM) and V_{max} (range 385 to 460 pmol/mg protein /min) (data not shown). However, the K_m and V_{max} values (0.5 ± 0.2 μM and 37 ± 9 pmol/mg/min, respectively) for the double Asn19/23Gln mutant were substantially decreased (Figure 4B and Table 1) and not significantly different from HeLa-WT-MRP1. This suggested that differences in glycosylation at Asn19 and Asn23 contributed to the differences in $As(GS)_3$ transport by HEK-WT-MRP1 and HeLa-WT-MRP1.

Kinetic analysis of $E_2$17βG transport by MRP1-Asn19/23Gln expressed in HEK293 cells. To ensure that, as for the fully glycosylated mutant, the Asn to Gln mutation of the first two glycosylation sites did not affect the transport affinity for every MRP1 substrate, $E_2$17βG kinetic parameters were determined for MRP1-Asn19/23Gln expressed in HEK293 cells (Figure 4C). The K_m value was 2.4 μM, similar to that previously published for HEK-WT-MRP1 and

Molecular Pharmacology Fast Forward. Published on June 13, 2016 as DOI: 10.1124/mol.116.103648
This article has not been copyedited and formatted. The final version may differ from this version.

HeLa-WT-MRP1 (Loe et al., 1996a; Stride et al., 1997) and determined for HEK-WT-MRP1, HEK-SF-MRP1, HeLa-WT-MRP1, and HeLa-SF-MRP1 by us (Figure 1C, 1D, 3C, and 3D). Thus, the effect of glycosylation on transport by MRP1 is substrate selective.

Kinetic analysis of As(GS)$_3$ transport by WT-MRP1 in the presence of phosphatase inhibitors. In parallel with the kinetic characterization of As(GS)$_3$ transport by SF-MRP1, the influence of phosphorylation was also investigated. Thus, kinetic parameters of As(GS)$_3$ transport by WT-MRP1-enriched membrane vesicles prepared in the presence of a PIC were determined. MRP1-enriched vesicles prepared from HeLa and HEK293 cells, in the presence of a PIC, displayed a high K_m (6.0 ± 1.3 µM and 3.6 ± 0.8 µM, respectively) and V_{max} (505 ± 292 pmol/mg/min and 270 ± 156 pmol/mg/min, respectively), parameters that are comparable to HEK-WT-MRP1 in the absence of PIC (Figure 5A, 5B, and Table 1). These results suggest that when MRP1 phosphorylation is maintained, MRP1 transports As(GS)$_3$ with lower affinity and higher capacity.

Kinetic analysis of As(GS)$_3$ transport by deglycosylated phosphorylated MRP1. To determine if the influence of glycosylation and phosphorylation on As(GS)$_3$ transport kinetics by MRP1were interdependent, K_m and V_{max} values were determined using SF- and Asn19/23Gln-MRP1-enriched membrane vesicles prepared in the presence of a PIC. Under these conditions, HeLa-SF-MRP1, HEK-SF-MRP1 and HEK-Asn19/23Gln-MRP1 enriched membrane vesicles had high K_m (3.2 ± 1.4 µM, 3.3 ± 1.8 µM, and 4.2 ± 1.6 µM, respectively) and high V_{max} (609 ± 251 pmol/mg/min, 195 ± 81 pmol/mg/min, and 300 ± 174 pmol/mg/min, respectively) values (Figure 5C, 5D, 5E, Table 1). These values were not significantly different from those for HEK-WT-MRP1 in the presence or absence of PIC. Therefore, maintaining phosphorylation of

Molecular Pharmacology Fast Forward. Published on June 13, 2016 as DOI: 10.1124/mol.116.103648
This article has not been copyedited and formatted. The final version may differ from this version.

deglycosylated MRP1 results in lower affinity, higher capacity transport of $As(GS)_3$, regardless of the cell line.

Effect of phosphorylation on limited trypsinolysis of deglycosylated MRP1. After demonstrating that the inclusion of a PIC during membrane vesicle preparation results in lower affinity, higher capacity transport of $As(GS)_3$ by WT-MRP1 and SF-MRP1 regardless of the cell type, experiments were designed to narrow the region of phosphorylation maintained in the presence of PIC. This was necessary because there are >50 predicted phospho-Ser, -Thr and Tyr sites in the cytosolic domains of MRP1 (NetPhos 2.0) (Blom et al., 1999). To do this we took advantage of the well characterized pattern of MRP1 fragments obtained after controlled exposure to trypsin and their detection with several regionally directed, MRP1-specific antibodies (Supplemental Figure 1A) (Hipfner et al., 1997; Mao et al., 2002). Thus, limited trypsinolysis was utilized to produce small molecular weight fragments of MRP1 to visualize mobility shifts, in the presence or absence of PIC, due to phosphorylation (Supplemental Figure 1). Tryptic fragments of MRP1 were detected with MRP1-specific antibodies against the NH_2-proximal (N1 and N2 with mAb MRPr1; N1 and N3 with pAb MRP-1) and COOH-proximal (C1 with mAb QCRL-1; C1 and C2 with mAb MRPm6) regions of the transporter (Supplemental Figure 1A).

Because of the striking difference between $As(GS)_3$ transport kinetics in vesicles prepared from HEK-SF-MRP1 in the presence and absence of PIC, the molecular weights of tryptic fragments of HEK-SF-MRP1 prepared under the two conditions were compared. As shown in Supplemental Figure 1B and C, a small shift in N1 mobility was detected with both MRPr1 and MRP-1 antibodies, suggesting that the N1 fragment contains a site that is phosphorylated when vesicles are prepared in the presence of PIC. Somewhat unexpectedly,

Molecular Pharmacology Fast Forward. Published on June 13, 2016 as DOI: 10.1124/mol.116.103648
This article has not been copyedited and formatted. The final version may differ from this version.

there was no detectable corresponding shift in the N2 (Supplemental Figure 1B) or N3 (Supplemental Figure 1C) fragments of HEK-SF-MRP1. These observations suggested that the phosphorylation site resided in the area of N1 cleaved between N2 and N3 or the cleaved COOH-terminal portion of N3 that are lost due to further trypsinolysis of the N2 and N3 fragments. Similar results to HEK-SF-MRP1 were obtained for HEK-N19/23Q-MRP1 in the presence and absence of PIC (data not shown). No shifts were observed for the C1 or C2 of the COOH-terminal fragments as detected with mAbs MRPm6 and QCRL-1 (data not shown). Taken together, the limited tryptic digest data suggested that the phosphorylated residues that are maintained by PIC treatment during membrane vesicle preparation reside within the N1 fragment and more specifically, in the regions cleaved by further trypsin digestion: CL3 connecting MSD0 to MSD1 and/or the linker region on the COOH-terminus of the NH_2-proximal half of MRP1 (Supplemental Figure 1A and Figure 6A).

Analysis of $As(GS)_3$ transport by MRP1 mutated at potential phosphorylation sites in CL3. To explore the possibility that phosphorylation of one or more amino acids in CL3 (spanning approximately amino acids 193-320) connecting MSD0 to MSD1 could be responsible for modulating the affinity and capacity of MRP1 for $As(GS)_3$, a site-directed mutagenesis based approach was employed. mAb MRPr1 reliably detects the N1 and N2 fragments (but not N3) after limited trypsinolysis of MRP1, indicating that its epitope remains intact during trypsin digestion. Therefore, if loss of a phosphorylation site between N2 and N3 during trypsinolysis occurs (as suggested by the results shown in Supplemental Figure 1B and C), it must occur COOH-proximal to Glu247 since the MRPr1 epitope has been mapped to amino acids 238-247 (Hipfner et al., 1998). There are seven Ser, three Thr and one Tyr residues between amino acids 248-320 of human MRP1. Ser304, Ser312, and Thr320 were excluded because they are located

Molecular Pharmacology Fast Forward. Published on June 13, 2016 as DOI: 10.1124/mol.116.103648
This article has not been copyedited and formatted. The final version may differ from this version.

far from the junction of the N2 and N3 fragments. To determine if the remaining Thr249, Ser250, Thr268, Tyr277, Ser278, Ser279, Ser288 and/or Ser289 were important for determining the affinity and capacity of MRP1 for $As(GS)_3$, they were individually mutated to Ala. All Ala-substituted mutants were expressed at comparable levels to WT-MRP1 in HEK293 cells (Figure 6). In addition, $As(GS)_3$ transport for all eight mutants exhibited high K_m (range 3.1 to 13 μM) and V_{max} (range 145 to 610 pmol/mg/min) values similar to those of HEK-WT-MRP1 (data not shown). To address the possibility that multiple residues in this region must be phosphorylated in order for a shift in kinetics to be observed, all eight potential phosphorylation sites were mutated in a single expression construct (i.e., MRP1-Thr249Ala/Ser 250Ala/Thr268Ala/ Tyr277Ala/ Ser278Ala/Ser279Ala/Ser288Ala/Ser289Ala or MRP1_8X_CL3). Characterization of $As(GS)_3$ kinetics for HEK-MRP1_8X_CL3 revealed moderately lower K_m of 2.0 ± 0.7 μM and V_{max} of 177 ± 90 pmol mg^{-1} protein min^{-1} values versus HEK-WT-MRP1; however, they were not significantly different. Thus, phosphorylation of the Ser/Thr/Tyr residues within CL3 did not account for the differences in $As(GS)_3$ transport kinetics between the HEK293 and HeLa cell lines.

Analysis of $As(GS)_3$ transport by MRP1 mutated at potential phosphorylation sites in the linker region between NBD1 and MSD2. To determine if the PIC-dependent shift in molecular weight of the N1 fragment of MRP1 (Supplemental Figure 1B and C) was due to phosphorylation at the COOH-terminus of NBD1, a site-directed mutagenesis study of this region was initiated. The linker region between NBD1 and MSD2 is hypersensitive to proteases and is also the site of the epitope detected by the MRP1-specific mAb QCRL-1 (amino acids 918-924) and thus represents the boundary between the N1 and C1 tryptic halves of MRP1 (Hipfner et al., 1996). Consequently, as a starting point eleven potential phosphorylation sites

Molecular Pharmacology Fast Forward. Published on June 13, 2016 as DOI: 10.1124/mol.116.103648
This article has not been copyedited and formatted. The final version may differ from this version.

between Ser905 to Thr931 were mutated either individually (Ser905Ala, Ser915Ala, Ser916Ala, Ser917Ala, Ser925Ala, Ser930Ala, Thr931Ala), or (to increase screening efficiency) as double mutants (Ser918/919Ala and Tyr920Phe/Ser921Ala). All single and double mutants were expressed at levels comparable to WT-MRP1 in HEK293 cells (Figure 6). The Ser916Ala and Thr931Ala mutants exhibited 1.3- and 1.5-fold higher $As(GS)_3$ (2.5 μM; 80 nCi) transport activity than WT-MRP1 (data not shown) and were not characterized kinetically. All other linker region mutants exhibited high K_m (range 2 to 5.7 μM) and V_{max} (range 81 to 323 pmol/mg protein/min) values similar to HEK-WT-MRP1 (data not shown), with one exception (Figure 7A, Table 2). Thus, the Tyr920Phe/Ser921Ala-MRP1 double mutant exhibited $As(GS)_3$ transport kinetic parameters (K_m of 0.4 ± 0.1 μM and V_{max} of 28 ± 16 pmol/mg/ min) very similar to HeLa-WT-MRP1 and HeLa/HEK-SF-MRP1, suggesting that phosphorylation of one or both of Tyr920 and Ser921 was critical for regulating the affinity and transport capacity of MRP1 for $As(GS)_3$.

To determine if phosphorylation of Tyr920, Ser921, or both were required for the shift in $As(GS)_3$ kinetic parameters, single mutants were generated and characterized (Table 2). The kinetic parameters for both single mutants Tyr920Phe-MRP1 (K_m of 3.9 ± 1.0 μM and V_{max} of 125 ± 54 pmol/mg/min) and Ser921Ala-MRP1 (K_m of 3.7 ± 1.3 μM and V_{max} of 122 ± 42 pmol/mg/ min) were higher than those of the double mutant and were not significantly different from HEK-WT-MRP1, suggesting that both Tyr920 and Ser921 must be mutated to observe the reduction of $As(GS)_3$ K_m and V_{max} values.

To mimic phosphorylation of Tyr920 and Ser921, both amino acids were also replaced with a negatively charged Glu residue. Consistent with phosphorylation of these amino acids being responsible for modulation of $As(GS)_3$ transport by MRP1, the HEK-Tyr920Glu/Ser921Glu-MRP1 exhibited $As(GS)_3$ transport kinetic parameters (K_m of 3.6 ± 0.8

Molecular Pharmacology Fast Forward. Published on June 13, 2016 as DOI: 10.1124/mol.116.103648
This article has not been copyedited and formatted. The final version may differ from this version.

μM and V_{max} of 135 ± 33 pmol/ mg/min) similar to those of HEK-WT-MRP1 (Table 2 and Figure 7B).

Transport of $E_2$17βG and methotrexate by HEK-Tyr920Phe/Ser921Ala-MRP1. To ensure that the double Tyr920Phe/Ser921Ala mutation did not just generally disrupt MRP1 function, kinetic parameters for $E_2$17βG transport by this mutant were determined. Similar to values determined for HeLa- and HEK-WT-MRP1 in this and previously published studies, $E_2$17βG was transported by HEK-Tyr920Phe/ Ser921Ala-MRP1 with a K_m of 2.3 μM and V_{max} of 424 pmol/ mg/min (compare Figure 7C with Figure 1C and 1D) (Loe et al., 1996a; Stride et al., 1997). Similarly, methotrexate (100 μM, 250 nCi) transport by HEK-Tyr920Phe/ Ser921Ala-MRP1 and WT-MRP1 were the same (Figure 7D). Methotrexate transport by the phosphorylation mimicking Tyr920Glu/ Ser921Glu-MRP1 mutant was also no different than WT-MRP1 (Figure 7D).

As(GS)$_3$ transport by HEK-Asn19/23Gln/Tyr920Glu/Ser921Glu-MRP1. To determine if the phosphorylation-mimicking Tyr920Glu/Ser921Glu substitutions could convert the Asn19/23Gln-MRP1 transport kinetics from a high affinity low capacity to lower affinity higher capacity transporter of As(GS)$_3$, the quadruple Asn19/23Gln/Tyr920Glu/Ser921Glu-MRP1 mutant was generated and expressed in HEK293 cells. Membrane vesicles enriched for this quadruple MRP1 mutant had kinetic parameters (K_m 6.4 ± 1.9 μM and V_{max} of 162 ± 58 pmol mg^{-1} protein min^{-1}) similar to HEK-WT-MRP1 (Figure 7E and Table 2), suggesting that the phosphorylation-mimicking substitutions restored the ability of the double *N*-glycosylation Asn19/23Gln mutant to transport As(GS)$_3$ with lower affinity and higher capacity. These results strongly suggest that it is phosphorylation of Tyr920 and Ser921, rather than *N*-glycosylation, that (directly) regulates As(GS)$_3$ transport capacity and affinity.

Molecular Pharmacology Fast Forward. Published on June 13, 2016 as DOI: 10.1124/mol.116.103648
This article has not been copyedited and formatted. The final version may differ from this version.

Effect of phosphorylation on immunoreactivity of MRP1 with mAb QCRL-1. Kinetic parameters for HeLa-WT-MRP1 were not significantly different from the dephosphorylated HEK-Tyr920Phe/Ser921Ala-MRP1 mutant, supporting the idea that HEK-WT-MRP1 and HeLa-WT-MRP1 are differentially phosphorylated at these amino acids (Tables 1 and 2). For this reason, the region of differential phosphorylation of HeLa-WT-MRP1 and HEK-WT-MRP1 was explored using the MRP1-specific mAb QCRL-1 whose epitope spans MRP1 amino acids 918-924 (and contains Tyr920 and Ser921) (Hipfner et al., 1996). Thus, immunoblots were done on samples prepared in the presence and absence of PIC to determine if the reactivity of QCRL-1 with HeLa-MRP1 and HEK-MRP1 vesicles was affected by phosphorylation (Supplemental Figure 2, top panel). These immunoblots were then stripped, treated with CIP and blotted again with QCRL-1 so that reactivity under the two conditions could be compared (Supplemental Figure 2, middle panel). Prior to CIP treatment, HEK-MRP1 levels were 60% lower than HeLa-MRP1 levels ($P < 0.02$) (Supplemental Figure 2, top panel). After CIP treatment, HEK-MRP1 levels were 5 ± 2-fold higher than HeLa-MRP1 levels ($P < 0.02$) (Supplemental Figure 2, middle panel). These results indicate that QCRL-1 reacts more strongly with dephosphorylated MRP1. They also strongly suggest that the region of MRP1 corresponding to the QCRL-1 epitope (918-924) in HEK293 and HeLa membrane vesicles is differentially phosphorylated. The difference in $As(GS)_3$ transport kinetics between HeLa-MRP1 prepared in the presence and absence of PIC was considerable, while no significant difference was observed under these conditions for HEK-MRP1 (Table 1). Importantly, the relative QCRL-1 reactivity was consistent with the relative differences in $As(GS)_3$ transport. Thus, prior to CIP treatment, HeLa-MRP1 (-PIC) levels were 1.7 ± 0.5-fold higher than HeLa-MRP1 (+PIC) levels ($P < 0.02$), indicating that HeLa-MRP1 (+PIC) QCRL-1 epitope was phosphorylated to a greater extent than HeLa-MRP1 (-PIC). After

Molecular Pharmacology Fast Forward. Published on June 13, 2016 as DOI: 10.1124/mol.116.103648
This article has not been copyedited and formatted. The final version may differ from this version.

CIP treatment and reprobing blots with QCRL-1, the difference in MRP1 signal intensity between HeLa-MRP1 (+PIC) and HeLa-MRP1 (-PIC) was lost. As observed for $As(GS)_3$ transport (Table 1, Figures 1B and 5B), there was no difference in QCRL-1 immunoreactivity between HEK-MRP1 with or without PIC (Supplementary Figure 2, top panel). Overall, these observations suggest that the QCRL-1 epitope (containing Tyr920/Ser921) is phosphorylated in HEK-MRP1 (±PIC) and HeLa-MRP1 (+PIC) to a greater extent than HeLa-MRP1 (-PIC), and under these conditions, higher $As(GS)_3$ K_m and V_{max} values are also observed.

Molecular Pharmacology Fast Forward. Published on June 13, 2016 as DOI: 10.1124/mol.116.103648
This article has not been copyedited and formatted. The final version may differ from this version.

DISCUSSION

The results presented in this study suggest that the substantial differences in the kinetics of $As(GS)_3$ transport by WT-MRP1-enriched membrane vesicles isolated from HEK293 and HeLa cells are caused by cell line specific differences in MRP1 post-translational modification. Specifically, MRP1 affinity and capacity for $As(GS)_3$ are influenced by glycosylation of Asn19 and Asn23 and phosphorylation of Tyr920 and Ser921. Our data also indicate that cross-talk occurs between MRP1 *N*-glycosylation and phosphorylation, with phosphorylation dictating the affinity and capacity for $As(GS)_3$, and *N*-glycosylation influencing the phosphorylation status. Finally, since transport of other organic anion substrates (i.e. $E_2$17βG and methotrexate) of MRP1 are unaffected by Tyr920/Ser921 phosphorylation, this post-translational regulation appears to be a substrate-selective phenomenon. We propose that phosphorylation of MRP1 at Tyr920 and Ser921 allows a switch from high affinity low capacity to low affinity high capacity resulting in the transport of arsenic by MRP1 over a wide concentration range.

The cell line differences in MRP1 transport kinetics for $As(GS)_3$ were unexpected because almost identical kinetic parameters had previously been reported using MRP1-enriched membrane vesicles isolated from HEK293 and HeLa cell lines for the prototypical MRP1 substrates $E_2$17βG and LTC_4 (Loe et al., 1996a; Loe et al., 1996b; Stride et al., 1997). Kinetic parameters of $E_2$17βG were also confirmed in this study to be very similar between the two cell lines (Figure 1C and D). Consistent with our observation that Tyr920 and Ser921 modulates MRP1 transport of $As(GS)_3$ selectively, amino acids 859 to 931 in the MRP1 linker region joining NBD1 to MSD2 have been shown previously to be non-essential for LTC_4 binding and transport (Gao et al., 1998). Furthermore, no difference was found for methotrexate transport activity between HEK-WT-MRP1 and the HEK-Tyr920Phe/Ser921Ala or HEK-

Molecular Pharmacology Fast Forward. Published on June 13, 2016 as DOI: 10.1124/mol.116.103648
This article has not been copyedited and formatted. The final version may differ from this version.

Tyr920Glu/Ser921Glu mutants (Figure 7D). Thus, our data support the conclusion that the $As(GS)_3$ binding site on MRP1 contains elements (i.e., contact amino acids) that distinguish it from the binding site(s) of not only $E_2$17βG and methotrexate, but also LTC_4, and likely other organic anions. This is consistent with previous reports that individual substrates of MRP1 establish their own distinct and often mutually exclusive interactions with amino acids (Cole and Deeley, 2006; Deeley and Cole, 2006; Maeno et al., 2009). Interestingly, casein kinase 2α-dependent phosphorylation of MRP1 at Thr249 in CL3 has been reported to stimulate the transport of LTC_4 and $E_2$17βG as well as reduce doxorubicin accumulation and cytotoxicity (Stolarczyk et al., 2012). In contrast, mutation of Thr249 to Ala had no significant effect on $As(GS)_3$ transport (K_m 5.1 ± 3.5 μM, V_{max} 404 ± 267 pmol/mg protein/min in HEK) providing further support for a unique $As(GS)_3$ binding site and a novel mechanism of MRP1 regulation. Kinases and phosphatases responsible for the phosphorylation and de-phosphorylation, respectively, of Tyr920 and Ser921 are potential therapeutic targets for increasing MRP1 function after environmental arsenic exposure or reducing MRP1 activity during As_2O_3 therapy.

Our finding that MRP1-Tyr920 is phosphorylated is in contrast to an earlier study in which phosphoamino acid analysis of MRP1 immunoprecipitated from HL60/ADR cells indicated that only Ser residues (but not Tyr or Thr residues) on the transporter are phosphorylated (Ma et al., 1995). The reasons for the different observations of the two studies are uncertain. However, Ma *et al.*, (Ma et al., 1995) included the protein tyrosine phosphatase (PTP) inhibitor sodium vanadate in their lysis buffer and since EDTA (a chelator of vanadate) was also present, PTP inhibition was likely incomplete (Huyer et al., 1997; Ma et al., 1995). Moreover, there are currently 70 records of MRP1-Tyr920 phosphorylation in the

Molecular Pharmacology Fast Forward. Published on June 13, 2016 as DOI: 10.1124/mol.116.103648
This article has not been copyedited and formatted. The final version may differ from this version.

PhosphoSitePlus database (www.PhosphositePlus.com) providing strong support for its utilization (Hornbeck et al., 2015).

Initially it was surprising to us that glycosylation influenced the affinity of MRP1 for $As(GS)_3$. Although *N*-linked glycosylation is well known to influence localization, stability and expression of a variety of membrane proteins, there are few examples of it affecting substrate binding by transporters (Filippo et al., 2011; Moremen et al., 2012; Scott and Panin, 2014). Our observation that SF-MRP1 and Asn19/23Gln-MRP1 membrane vesicles prepared in the presence of a PIC had low affinity high capacity $As(GS)_3$ transport regardless of the cell line from which they were prepared suggested that glycosylation might be influencing the phosphorylation status of MRP1 rather than directly altering $As(GS)_3$ affinity and capacity. Membrane vesicles prepared from Asn19/23Gln/Tyr920Glu/Ser 921Glu-MRP1expressed in HEK293 cells had low affinity high capacity $As(GS)_3$ transport (Figure 7E and Table 2), consistent with phosphorylation dictating MRP1's $As(GS)_3$ affinity and capacity rather than glycosylation.

How glycosylation of Asn19 and Asn23 at the extracellular NH_2-terminus of MRP1 influences Tyr920 and Ser921 phosphorylation in the cytosolic linker region between NBD1 and MSD2 remains to be determined. One possibility is that the size and content of the glycans at the NH_2-terminus could influence the conformation of MRP1 and alter the accessibility of its linker region to kinases and/or phosphatases. Indeed, some evidence has been reported suggesting that the intracellular domains can influence the extracellular NH_2-terminus of MRP1. For example, evidence from antibody binding to the NH_2-terminus suggests that ATP-binding to the cytosolic NBDs of MRP1 results in a conformational change propagated to the NH_2-terminal domain (Binyamin et al., 2005). Interestingly, reduced *N*-linked glycosylation of MRP1 has been reported in an oxaliplatin selected ovarian carcinoma cell line relative to its parental cell

Molecular Pharmacology Fast Forward. Published on June 13, 2016 as DOI: 10.1124/mol.116.103648
This article has not been copyedited and formatted. The final version may differ from this version.

line (Beretta et al., 2010). The sugar group content of glycosylation has been reported to differ for other *N*-glycosylated proteins between different cell/tissue types and during disease states (Bull et al., 2014; Ferris et al., 2014; Fujikura et al., 2011; Fujimori-Arai et al., 1997; Peng et al., 2003). Thus, it is possible that the composition of MRP1 glycosylation could vary between different healthy tissue types and/or different disease states, which in turn could alter MRP1 phosphorylation at Tyr920 and Ser921. This has the potential to ultimately impact the detoxification of arsenic as well as any other (yet to be identified) substrates that involve Tyr920 and Ser921 in MRP1 for binding and transport.

The relative resistance of HEK293 and HeLa cells stably expressing MRP1 to As^{III} is similar (~2- and 3-fold, respectively) (Carew et al., 2011; Cole et al., 1994; Stride et al., 1997), suggesting that phosphorylation of Tyr920 and Ser921 may occur to the same extent in the two cell lines under certain conditions. This is consistent with the presence of PIC during the vesicle preparation resulting in low affinity high capacity $As(GS)_3$ transport function, regardless of the cell line. Thus, although the kinases responsible for Tyr920 and Ser921 phosphorylation are important to identify, we think it is more likely that the differences between HEK-WT-MRP1 and HeLa-WT-MRP1 membrane vesicles are caused by differences in susceptibility to a phosphatase, potentially as a result of a conformation change in the linker region induced by differential glycosylation.

It is also possible that the HEK293 and HeLa cells express different phosphatases and HEK-WT-MRP1 retains Tyr920 and Ser921 phosphorylation because the appropriate phosphatase(s) responsible for cleaving these sites is/are not expressed. Interestingly, multiple studies have shown that arsenic can influence both kinase and phosphatase signalling pathways. For example, arsenic can activate mitogen activated protein kinase (MAPK), JNK kinase, and

Molecular Pharmacology Fast Forward. Published on June 13, 2016 as DOI: 10.1124/mol.116.103648
This article has not been copyedited and formatted. The final version may differ from this version.

PI3K/Akt/mTOR pathways (Beauchamp et al., 2015; Giafis et al., 2006; Goussetis and Platanias, 2010; Platanias, 2009; Verma et al., 2002). Phosphoproteomic studies comparing untreated and arsenic treated cell lines have also shown a general increase in protein phosphorylation through these pathways (Alp et al., 2010; Wen et al., 2010). Arsenic is also known to inhibit certain phosphatases including protein tyrosine phosphatase 1B and the transmembrane tyrosine phosphatase CD45 (Rehman et al., 2012). Thus, we suggest that exposure of cells to arsenic results in a shift to a pro-phosphorylation state which in turn promotes MRP1 to switch from a high affinity low capacity to a low affinity high capacity $As(GS)_3$ transporter.

The success of As_2O_3 in the treatment of acute promyelocytic leukemia has generated substantial interest in its use as a therapeutic for other leukemias and solid tumours (Platanias, 2009; Subbarayan and Ardalan, 2014). *In vitro* results are promising, but clinical success has been limited by the higher doses of As_2O_3 required for induction of non-APL tumour cell death (Platanias, 2009). Considerable effort has been made to target kinase pathways that are activated by As_2O_3 to increase the efficacy of this agent (Beauchamp et al., 2015; Dolniak et al., 2008; Galvin et al., 2013; Giafis et al., 2006; Lozano-Santos et al., 2015; McNeer et al., 2010; Verma et al., 2002). It may be that the kinase pathways responsible for phosphorylation of Tyr920 and Ser921 of MRP1 overlap with the kinase pathways activated by As_2O_3. If this is true then the administration of kinase inhibitors would not only increase the anti-leukemic properties of As_2O_3, but would also prevent Tyr920 and Ser921 phosphorylation, resulting in saturation of MRP1 transport and increased As_2O_3 accumulation within tumour cells.

In conclusion, the results of the present study show that *N*-glycosylation and Ser/Tyr phosphorylation are critical for the regulation of MRP1-mediated transport of $As(GS)_3$ and could considerably alter handling of arsenic by cells and tissues. Thus, phosphorylation of MRP1

Molecular Pharmacology Fast Forward. Published on June 13, 2016 as DOI: 10.1124/mol.116.103648
This article has not been copyedited and formatted. The final version may differ from this version.

presents a novel and potential high impact cellular defense mechanism, based on its ability to switch cellular arsenic efflux from a high affinity low capacity process (important during low levels of arsenic exposure), to a lower affinity but higher capacity process under conditions of higher arsenic exposure. Our findings have important implications for the future design of therapeutic agents that can modulate the phosphorylation status of MRP1 to increase its transport capacity during arsenic poisoning and reduce its transport capacity during administration of arsenic-based chemotherapeutics.

Molecular Pharmacology Fast Forward. Published on June 13, 2016 as DOI: 10.1124/mol.116.103648
This article has not been copyedited and formatted. The final version may differ from this version.

ACKNOWLEDGEMENTS

The authors would like to thank Brayden Whitlock for technical assistance.

Molecular Pharmacology Fast Forward. Published on June 13, 2016 as DOI: 10.1124/mol.116.103648
This article has not been copyedited and formatted. The final version may differ from this version.

AUTHORSHIP CONTRIBUTIONS

Participated in research design: Shukalek and Leslie

Conducted experiments: Shukalek, Swanlund, Rousseau, and Marensi

Contributed new reagents or analytic tools: Shukalek, Swanlund, Rousseau, Weigl, Cole, and Leslie

Performed data analysis: Shukalek, Swanlund, and Leslie

Wrote or contributed to the writing of the manuscript: Shukalek, Cole, and Leslie

REFERENCES

Almquist KC, Loe DW, Hipfner DR, Mackie JE, Cole SP and Deeley RG (1995) Characterization of the M(r) 190,000 multidrug resistance protein (MRP) in drug-selected and transfected human tumor cell. *Cancer Res* **55**:102-110.

Alp O, Merino EJ and Caruso JA (2010) Arsenic-induced protein phosphorylation changes in HeLa cells. *Anal Bioanal Chem* **398**:2099-2107.

Banerjee M, Carew MW, Roggenbeck BA, Whitlock BD, Naranmandura H, Le XC and Leslie EM (2014) A Novel Pathway for Arsenic Elimination: Human Multidrug Resistance Protein 4 (MRP4/ABCC4) Mediates Cellular Export of Dimethylarsinic Acid (DMAV) and the Diglutathione Conjugate of Monomethylarsonous Acid (MMAIII). *Mol Pharmacol* **86**:168-179.

Beauchamp EM, Kosciuczuk EM, Serrano R, Nanavati D, Swindell EP, Viollet B, O'Halloran TV, Altman JK and Platanias LC (2015) Direct binding of arsenic trioxide to AMPK and generation of inhibitory effects on acute myeloid leukemia precursors. *Mol Cancer Ther* **14**:202-212.

Beretta GL, Benedetti V, Cossa G, Assaraf YG, Bram E, Gatti L, Corna E, Carenini N, Colangelo D, Howell SB, Zunino F and Perego P (2010) Increased levels and defective glycosylation of MRPs in ovarian carcinoma cells resistant to oxaliplatin. *Biochem Pharmacol* **79**:1108-1117.

Binyamin L, Assaraf YG and Reiter Y (2005) Probing ATP-dependent conformational changes in the multidrug resistance protein 1 (MRP1/ABCC1) in live tumor cells with a novel

recombinant single-chain Fv antibody targeted to the extracellular N-terminus. *Int J Cancer* **116**:703-709.

Blom N, Gammeltoft S and Brunak S (1999) Sequence and structure-based prediction of eukaryotic protein phosphorylation sites. *J Mol Biol* **294**:1351-1362.

Bull C, Stoel MA, den Brok MH and Adema GJ (2014) Sialic acids sweeten a tumor's life. *Cancer Res* **74**:3199-3204.

Carew MW and Leslie EM (2010) Selenium-dependent and -independent transport of arsenic by the human multidrug resistance protein 2 (MRP2/ABCC2): implications for the mutual detoxification of arsenic and selenium. *Carcinogenesis* **31**:1450-1455.

Carew MW, Naranmandura H, Shukalek CB, Le XC and Leslie EM (2011) Monomethylarsenic diglutathione transport by the human multidrug resistance protein 1 (MRP1/ABCC1). *Drug Metab Dispos* **39**:2298-2304.

Chen CA and Okayama H (1988) Calcium phosphate-mediated gene transfer: a highly efficient transfection system for stably transforming cells with plasmid DNA. *Biotechniques* **6**:632-638.

Cole SP (2013) Targeting Multidrug Resistance Protein 1 (MRP1, ABCC1): Past, Present, and Future. *Annu Rev Pharmacol Toxicol* **54**:95-117.

Cole SP (2014) Multidrug resistance protein 1 (MRP1, ABCC1), a "multitasking" ATP-binding cassette (ABC) transporter. *J Biol Chem* **289**:30880-30888.

Cole SP and Deeley RG (2006) Transport of glutathione and glutathione conjugates by MRP1. *Trends Pharmacol Sci* **27**:438-446.

Cole SP, Sparks KE, Fraser K, Loe DW, Grant CE, Wilson GM and Deeley RG (1994) Pharmacological characterization of multidrug resistant MRP-transfected human tumor cells. *Cancer Res* **54**:5902-5910.

Deeley RG and Cole SP (2006) Substrate recognition and transport by multidrug resistance protein 1 (ABCC1). *FEBS Lett* **580**:1103-1111.

Dolniak B, Katsoulidis E, Carayol N, Altman JK, Redig AJ, Tallman MS, Ueda T, Watanabe-Fukunaga R, Fukunaga R and Platanias LC (2008) Regulation of arsenic trioxide-induced cellular responses by Mnk1 and Mnk2. *J Biol Chem* **283**:12034-12042.

Drobna Z, Walton FS, Paul DS, Xing W, Thomas DJ and Styblo M (2010) Metabolism of arsenic in human liver: the role of membrane transporters. *Arch Toxicol* **84**:3-16.

Ferris SP, Kodali VK and Kaufman RJ (2014) Glycoprotein folding and quality-control mechanisms in protein-folding diseases. *Dis Model Mech* **7**:331-341.

Filippo CA, Ardon O and Longo N (2011) Glycosylation of the OCTN2 carnitine transporter: study of natural mutations identified in patients with primary carnitine deficiency. *Biochim Biophys Acta* **1812**:312-320.

Fujikura Y, Krijt J and Necas E (2011) Liver and muscle hemojuvelin are differently glycosylated. *BMC biochemistry* **12**:52.

Fujimori-Arai Y, Koyama I, Hirano K and Komoda T (1997) Intestinal alkaline phosphatase isoforms in rabbit tissues differ in glycosylation patterns. *Clin Biochem* **30**:545-551.

Galvin JP, Altman JK, Szilard A, Goussetis DJ, Vakana E, Sassano A and Platanias LC (2013) Regulation of the kinase RSK1 by arsenic trioxide and generation of antileukemic responses. *Cancer Biol Ther* **14**:411-416.

Gao M, Yamazaki M, Loe DW, Westlake CJ, Grant CE, Cole SP and Deeley RG (1998) Multidrug resistance protein. Identification of regions required for active transport of leukotriene C4. *J Biol Chem* **273**:10733-10740.

Garelick H, Jones H, Dybowska A and Valsami-Jones E (2008) Arsenic pollution sources. *Rev Environ Contam Toxicol* **197**:17-60.

Giafis N, Katsoulidis E, Sassano A, Tallman MS, Higgins LS, Nebreda AR, Davis RJ and Platanias LC (2006) Role of the p38 mitogen-activated protein kinase pathway in the generation of arsenic trioxide-dependent cellular responses. *Cancer Res* **66**:6763-6771.

Goussetis DJ and Platanias LC (2010) Arsenic trioxide and the phosphoinositide 3-kinase/akt pathway in chronic lymphocytic leukemia. *Clin Cancer Res* **16**:4311-4312.

Hipfner DR, Almquist KC, Leslie EM, Gerlach JH, Grant CE, Deeley RG and Cole SP (1997) Membrane topology of the multidrug resistance protein (MRP). A study of glycosylation-site mutants reveals an extracytosolic NH2 terminus. *J Biol Chem* **272**:23623-23630.

Hipfner DR, Almquist KC, Stride BD, Deeley RG and Cole SP (1996) Location of a protease-hypersensitive region in the multidrug resistance protein (MRP) by mapping of the epitope of MRP-specific monoclonal antibody QCRL-1. *Cancer Res* **56**:3307-3314.

Hipfner DR, Gao M, Scheffer G, Scheper RJ, Deeley RG and Cole SP (1998) Epitope mapping of monoclonal antibodies specific for the 190-kDa multidrug resistance protein (MRP). *Br J Cancer* **78**:1134-1140.

Hipfner DR, Gauldie SD, Deeley RG and Cole SP (1994) Detection of the M(r) 190,000 multidrug resistance protein, MRP, with monoclonal antibodies. *Cancer Res* **54**:5788-5792.

Hornbeck PV, Zhang B, Murray B, Kornhauser JM, Latham V and Skrzypek E (2015) PhosphoSitePlus, 2014: mutations, PTMs and recalibrations. *Nucleic Acids Res* **43**:D512-520.

Huyer G, Liu S, Kelly J, Moffat J, Payette P, Kennedy B, Tsaprailis G, Gresser MJ and Ramachandran C (1997) Mechanism of inhibition of protein-tyrosine phosphatases by vanadate and pervanadate. *J Biol Chem* **272**:843-851.

IARC (2012) A review of human carcinogens: Arsenic, Metals, Fibres and Dusts.

Ito K, Olsen SL, Qiu W, Deeley RG and Cole SP (2001) Mutation of a single conserved tryptophan in multidrug resistance protein 1 (MRP1/ABCC1) results in loss of drug resistance and selective loss of organic anion transport. *J Biol Chem* **276**:15616-15624.

Jedlitschky G, Leier I, Buchholz U, Barnouin K, Kurz G and Keppler D (1996) Transport of glutathione, glucuronate, and sulfate conjugates by the MRP gene-encoded conjugate export pump. *Cancer Res* **56**:988-994.

Kala SV, Kala G, Prater CI, Sartorelli AC and Lieberman MW (2004) Formation and urinary excretion of arsenic triglutathione and methylarsenic diglutathione. *Chem Res Toxicol* **17**:243-249.

Kala SV, Neely MW, Kala G, Prater CI, Atwood DW, Rice JS and Lieberman MW (2000) The MRP2/cMOAT transporter and arsenic-glutathione complex formation are required for biliary excretion of arsenic. *J Biol Chem* **275**:33404-33408.

Kritharis A, Bradley TP and Budman DR (2013) The evolving use of arsenic in pharmacotherapy of malignant disease. *Ann Hematol* **92**:719-730.

Leslie EM (2012) Arsenic-glutathione conjugate transport by the human multidrug resistance proteins (MRPs/ABCCs). *J Inorg Biochem* **108**:141-149.

Leslie EM, Deeley RG and Cole SP (2005) Multidrug resistance proteins: role of P-glycoprotein, MRP1, MRP2, and BCRP (ABCG2) in tissue defense. *Toxicol Appl Pharmacol* **204**:216-237.

Leslie EM, Haimeur A and Waalkes MP (2004) Arsenic transport by the human multidrug resistance protein 1 (MRP1/ABCC1). Evidence that a tri-glutathione conjugate is required. *J Biol Chem* **279**:32700-32708.

Loe DW, Almquist KC, Cole SP and Deeley RG (1996a) ATP-dependent 17 beta-estradiol 17-(beta-D-glucuronide) transport by multidrug resistance protein (MRP). Inhibition by cholestatic steroids. *J Biol Chem* **271**:9683-9689.

Loe DW, Almquist KC, Deeley RG and Cole SP (1996b) Multidrug resistance protein (MRP)-mediated transport of leukotriene C_4 and chemotherapeutic agents in membrane vesicles. Demonstration of glutathione-dependent vincristine transport. *J Biol Chem* **271**:9675-9682.

Lozano-Santos C, Amigo-Jimenez I, Nova-Gurumeta S, Perez-Sanz N, Garcia-Pardo A and Garcia-Marco JA (2015) Arsenic trioxide synergistically potentiates the cytotoxic effect of fludarabine in chronic lymphocytic leukemia cells by further inactivating the Akt and ERK signaling pathways. *Biochem Biophys Res Commun* **461**:243-248.

Ma L, Krishnamachary N and Center MS (1995) Phosphorylation of the multidrug resistance associated protein gene encoded protein P190. *Biochemistry* **34**:3338-3343.

Maeno K, Nakajima A, Conseil G, Rothnie A, Deeley RG and Cole SP (2009) Molecular basis for reduced estrone sulfate transport and altered modulator sensitivity of transmembrane helix (TM) 6 and TM17 mutants of multidrug resistance protein 1 (ABCC1). *Drug Metab Dispos* **37**:1411-1420.

Mao Q, Qiu W, Weigl KE, Lander PA, Tabas L, Shepard RL, Dantzig AH, Deeley RG and Cole SP (2002) GSH-Dependent photolabeling of multidrug resistance protein MRP1 (ABCC1) by [125I]-LY475776: Evidence of a major binding site in the COOH-proximal membrane spanning domain. *J Biol Chem* **277**:28690-28699.

Mass MJ, Tennant A, Roop BC, Cullen WR, Styblo M, Thomas DJ and Kligerman AD (2001) Methylated trivalent arsenic species are genotoxic. *Chem Res Toxicol* **14**:355-361.

McNeer JL, Goussetis DJ, Sassano A, Dolniak B, Kroczynska B, Glaser H, Altman JK and Platanias LC (2010) Arsenic trioxide-dependent activation of thousand-and-one amino acid kinase 2 and transforming growth factor-beta-activated kinase 1. *Mol Pharmacol* **77**:828-835.

Moremen KW, Tiemeyer M and Nairn AV (2012) Vertebrate protein glycosylation: diversity, synthesis and function. *Nat Rev Mol Cell Biol* **13**:448-462.

Mukhopadhyay R, Bhattacharjee H and Rosen BP (2014) Aquaglyceroporins: generalized metalloid channels. *Biochim Biophys Acta* **1840**:1583-1591.

Peng Q, McEuen AR, Benyon RC and Walls AF (2003) The heterogeneity of mast cell tryptase from human lung and skin. *Eur J Biochem* **270**:270-283.

Petrick JS, Ayala-Fierro F, Cullen WR, Carter DE and Vasken Aposhian H (2000) Monomethylarsonous acid (MMA(III)) is more toxic than arsenite in Chang human hepatocytes. *Toxicol Appl Pharmacol* **163**:203-207.

Platanias LC (2009) Biological responses to arsenic compounds. *J Biol Chem* **284**:18583-18587.

Ramirez-Solis A, Mukopadhyay R, Rosen BP and Stemmler TL (2004) Experimental and theoretical characterization of arsenite in water: insights into the coordination environment of As-O. *Inorg Chem* **43**:2954-2959.

Reay PF and Asher CJ (1977) Preparation and purification of 74As-labeled arsenate and arsenite for use in biological experiments. *Anal Biochem* **78**:557-560.

Rehman K, Chen Z, Wang WW, Wang YW, Sakamoto A, Zhang YF, Naranmandura H and Suzuki N (2012) Mechanisms underlying the inhibitory effects of arsenic compounds on protein tyrosine phosphatase (PTP). *Toxicol Appl Pharmacol* **263**:273-280.

Scott H and Panin VM (2014) The role of protein N-glycosylation in neural transmission. *Glycobiology* **24**:407-417.

Shukalek CB and Leslie EM (2011) Arsenic triglutathione transport by wild-type, Cys43Ser, and Cys265Ser human multidrug resistance protein 1 (MRP1/ABCC1). *Biochem Cell Biol* **89**:264.

Stolarczyk EI, Reiling CJ, Pickin KA, Coppage R, Knecht MR and Paumi CM (2012) Casein kinase 2alpha regulates multidrug resistance-associated protein 1 function via phosphorylation of Thr249. *Mol Pharmacol* **82**:488-499.

Stride BD, Grant CE, Loe DW, Hipfner DR, Cole SP and Deeley RG (1997) Pharmacological characterization of the murine and human orthologs of multidrug resistance protein in transfected human embryonic kidney cells. *Mol Pharmacol* **52**:344-353.

Subbarayan PR and Ardalan B (2014) In the war against solid tumors arsenic trioxide needs partners. *J Gastrointest Cancer* **45**:363-371.

Verma A, Mohindru M, Deb DK, Sassano A, Kambhampati S, Ravandi F, Minucci S, Kalvakolanu DV and Platanias LC (2002) Activation of Rac1 and the p38 mitogen-activated protein kinase pathway in response to arsenic trioxide. *J Biol Chem* **277**:44988-44995.

Villa-Bellosta R and Sorribas V (2010) Arsenate transport by sodium/phosphate cotransporter type IIb. *Toxicol Appl Pharmacol* **247**:36-40.

Weigl KE (2005) Biochemical investigations of the human multidrug resistance protein 1 (MRP1/ABCC1): analysis of *N*-glycosylation and topology, Queen's University, Kingston.

Wen G, Hong M, Calaf GM, Roy D, Partridge MA, Li B and Hei TK (2010) Phosphoproteomic profiling of arsenite-treated human small airway epithelial cells. *Oncol Rep* **23**:405-412.

Molecular Pharmacology Fast Forward. Published on June 13, 2016 as DOI: 10.1124/mol.116.103648
This article has not been copyedited and formatted. The final version may differ from this version.

FOOTNOTES

This work was supported by the Canadian Institutes of Health Research [grant numbers MOP-272075, 84218, 106513, and 133584] and the Alberta Cancer Foundation [grant number 25842]. CBS was supported by a CIHR Frederick Banting and Charles Best Canada Graduate Scholarship. SPCC is the Queen's University Bracken Chair in Genetics and Molecular Medicine and Canada Research Chair in Cancer Biology. EML is an Alberta Innovates Health Solutions Scholar and was a CIHR New Investigator.

Address correspondence to: Dr. Elaine M. Leslie, 7-08A Medical Sciences Building, Department of Physiology, University of Alberta, Edmonton, AB, Canada, T6G 2H7; Email: eleslie@ualberta.ca; Tel: (780) 492-9250; Fax: (780) 248-1995.

CBS current address: Department of Medicine, Cummings School of Medicine, University of Calgary, Calgary, AB, Canada

RKR current address: Department of Immunology, University of Toronto, Toronto, ON, Canada

Molecular Pharmacology Fast Forward. Published on June 13, 2016 as DOI: 10.1124/mol.116.103648
This article has not been copyedited and formatted. The final version may differ from this version.

FIGURE LEGENDS

Figure 1: Kinetic analysis of $As(GS)_3$ and $E_2$17βG transport by WT-MRP1 enriched membrane vesicles prepared from HeLa and HEK293 cells. ATP-dependent uptake of (A, B) $As(GS)_3$ (0.05 – 20 µM, 30-120 nCi) or (C, D) $E_2$17βG (0.1 – 30 µM, 30-80 nCi) was measured for 1 and 1.5 min, respectively, at 37°C using membrane vesicles prepared from (A, C) HeLa-WT-MRP1 or (B, D) HEK-WT-MRP1 cells. Kinetic values were determined using Michaelis-Menten non-linear regression analysis (Graphpad Prism). Data points represent means (+ SD) of triplicate determinations in a single experiment. Similar results were obtained in at least two additional independent experiments and mean kinetic parameters for $As(GS)_3$ transport are summarized in Table 1. All data were corrected for MRP1 levels relative to HEK-WT-MRP1.

Figure 2: Glycosylation status of WT-MRP1 stably expressed in HEK293 and HeLa cells. Plasma membrane preparations from WT-MRP1 expressed in HEK293 and HeLa cells were incubated with or without the deglycosylation enzymes, Endo H and PNGaseF, separated by 8% SDS-PAGE and immunoblotted with the anti-MRP1 specific rat mAb MRPr1 (epitope mapped to amino acids 238-247) (Hipfner et al., 1998). The sugar free (SF)-MRP1 mutant was included as a control for comparison purposes.

Figure 3: Kinetics of $As(GS)_3$ and $E_2$17βG transport by SF-MRP1 enriched membrane vesicles prepared from HeLa and HEK293 cells. ATP-dependent uptake of (A, B) $As(GS)_3$ (0.05 – 10 µM, 30-120 nCi) or (C, D) $E_2$17βG (0.1 – 30 µM, 30-80 nCi) was measured for 1 min and 1.5 min, respectively, at 37°C using membrane vesicles prepared from (A, C) HeLa-SF-MRP1 or (B, D) HEK-SF-MRP1 cells. Kinetic values were determined using Michaelis-Menten non-linear regression analysis (Graphpad Prism). Data points represent means (+ SD) of triplicate determinations in a single experiment and were

Molecular Pharmacology Fast Forward. Published on June 13, 2016 as DOI: 10.1124/mol.116.103648
This article has not been copyedited and formatted. The final version may differ from this version.

corrected for MRP1 levels relative to HEK-WT-MRP1. For (A, B) similar results were obtained in at least 3 additional experiments and mean kinetic parameters for $As(GS)_3$ transport are summarized in Table 1.

Figure 4: Expression of MRP1 glycosylation mutants in HEK293 cells and kinetic analysis of $As(GS)_3$ and $E_2$17βG transport by MRP1-N19/23Q. (A) Plasma membrane enriched fractions containing various *N*-linked glycosylation site mutants of MRP1 were resolved by 7% SDS-PAGE, immunoblotted with the anti-MRP1 specific mAb MRPr1. Blots were then probed with the anti-Na^+/K^+-ATPase specific pAb H-300. A hatched line is present to emphasize the slight shift in molecular weight between the WT-MRP1 and the glycosylation mutants. (B and C) MRP1-N19/23Q enriched plasma membrane vesicles prepared from HEK293 cells were used to measure transport of (B) $As(GS)_3$ (0.05 – 2.5 μM, 30-80 nCi) and (C) $E_2$17βG (0.1 – 30 μM, 30-80 nCi) at 1 min and 1.5 min, respectively at 37°C. Kinetic values were determined using Michaelis-Menten non-linear regression analysis (Graphpad Prism). Data points represent means (+ SD) in a single experiment and similar results were obtained in two additional experiments with mean kinetic parameters for $As(GS)_3$ transport summarized in Table 1. All data were corrected for MRP1 levels relative to HEK-WT-MRP1.

Figure 5: Kinetics of $As(GS)_3$ transport by WT-MRP1, SF-MRP1 and N19/23Q-MRP1 enriched membrane vesicles prepared in the presence of a phosphatase inhibitor cocktail (PIC) from HeLa and/or HEK293 cells. $As(GS)_3$ (0.05 – 30 μM, 30-120 nCi) transport by MRP1 enriched membrane vesicles prepared in the presence of a PIC from (A) HeLa-WT-MRP1, (B) HEK-WT-MRP1, (C) HeLa-SF-MRP1, (D) HEK-SF-MRP1, and (E) HEK-N19/23Q-MRP1 was measured for 1 min at 37°C. Kinetic values were determined using Michaelis-Menten non-linear regression analysis (Graphpad Prism). Data points represent means (+ SD) in a single experiment and similar results were obtained in at least two additional experiments. Mean kinetic parameters are summarized in Table 1. All data were corrected for MRP1 levels relative to HEK-WT-MRP1.

Molecular Pharmacology Fast Forward. Published on June 13, 2016 as DOI: 10.1124/mol.116.103648
This article has not been copyedited and formatted. The final version may differ from this version.

Figure 6: Predicted location of selected potential Ser/Thr/Tyr phosphorylation sites in human MRP1 and immunoblots of MRP1 mutated at these residues. (A) Shown is a predicted secondary structure of MRP1. The locations of the 19 potential phosphorylation sites mutated in this study are indicated. (B and C) Shown are representative immunoblots of membrane vesicles prepared from HEK293 cells expressing empty vector, WT-MRP1, and potential single and double phosphorylation site MRP1 mutants: (B) CL3 mutants; or (C) mutants in the linker region between NBD1 and MSD2. MRP1 proteins were detected with mAb MRPm6 and then blots stripped and probed with the anti-Na^+/K^+-ATPase antibody H-300 (as a loading control).

Figure 7: $As(GS)_3$, $E_2 17\beta G$ and/or methotrexate transport by Tyr920Phe/Ser921Ala-MRP1, Tyr920Glu/Ser921Glu-MRP1, and Asn19/23Gln/Tyr920Glu/Ser921Glu –MRP1 enriched membrane vesicles prepared from HEK293 cells. ATP-dependent uptake of (A, B, and E) $As(GS)_3$ (0.05 – 20 μM), (C) $E_2 17\beta G$ (0.1 – 30 μM, 30-80 nCi) or (D) methotrexate (100 μM, 250 nCi) was measured for 1, 1.5 and 20 min respectively, at 37°C using membrane vesicles prepared from HEK293 cells expressing the indicated *N*-glycosylation and phosphomimetic mutant MRP1 proteins. Data points and bars represent means (+ SD) of triplicate determinations in a single experiment and similar results were obtained in at least one additional experiment. All data were corrected for MRP1 levels relative to HEK-WT-MRP1. Kinetic values were determined using Michaelis-Menten non-linear regression analysis (Graphpad Prism). Mean kinetic parameters for $As(GS)_3$ transport are summarized in Table 2.

Molecular Pharmacology Fast Forward. Published on June 13, 2016 as DOI: 10.1124/mol.116.103648
This article has not been copyedited and formatted. The final version may differ from this version.

TABLES

Table 1: Summary of kinetic values of $As(GS)_3$ transport by WT-MRP1, SF-MRP1, and Asn19/23Gln-MRP1 enriched membrane vesicles from HeLa and HEK293 cells prepared in the presence or absence of a phosphatase inhibitor cocktail (PIC).

	K_m ± SD (μM)	[a]V_{max} ± SD (pmol mg^{-1} min^{-1})	*N*
HeLa			
WT-MRP1	0.32 ± 0.03*	42 ± 17**	4
WT-MRP1 + PIC	6.0 ± 1.3	505 ± 292	3
SF-MRP1	0.3 ± 0.1*	44 ± 15**	5
SF-MRP1 + PIC	3.2 ± 1.4	609 ± 251	5
HEK293			
WT-MRP1	3.8 ± 1.2	307 ± 118	8
WT-MRP1 + PIC	3.6 ± 0.8	270 ± 156	4
SF-MRP1	0.6 ± 0.4*	38 ± 21**	4
SF-MRP1 + PIC	3.3 ± 1.8	195 ± 81	5
Asn19/23Gln-MRP1	0.5 ± 0.2*	37 ± 9**	3
Asn19/23Gln-MRP1 + PIC	4.2 ± 1.6	300 ± 174	6

[a]V_{max} values were corrected for levels of WT-MRP1, SF-MRP1 and Asn19/23Gln relative to HEK-WT-MRP1 using densitometry (ImageJ) analysis of at least 3 different immunoblots (see Supplementary Table 2).

*K_m value significantly different ($P < 0.01$) than for HEK-WT-MRP1 (one way ANOVA, Dunnett's multiple comparison test)

**V_{max} value significantly different ($P < 0.01$) than for HEK-WT-MRP1 (one way ANOVA, Dunnett's multiple comparison test)

Molecular Pharmacology Fast Forward. Published on June 13, 2016 as DOI: 10.1124/mol.116.103648
This article has not been copyedited and formatted. The final version may differ from this version.

Table 2: Summary of $As(GS)_3$ transport kinetic parameters for HEK-MRP1 mutated at Tyr920 and Ser921.

	K_m (± SD) (μM)	V_{max} (corrected)[a] (± SD) (pmol mg^{-1} min^{-1})	*N*
WT	3.8 ± 1.2	307 ± 118	8
Y920F/S921A	0.4 ± 0.1*	28 ± 16**	3
Y920F	3.9 ± 1.0	125 ± 54	3
S921A	3.7 ± 1.3	122 ± 42	3
Y920E/S921E	3.6 ± 0.8	135 ± 33	4
N19/23Q/Y920E/S921E	6.4 ± 1.9	162 ± 58	5

[a]V_{max} values were corrected for levels of mutant MRP1 relative to WT-MRP1 using densitometry (ImageJ) of at least 3 different immunoblots (see Supplementary Table 2).

*K_m value significantly different ($P < 0.01$) than for HEK-WT-MRP1 (one way ANOVA, Dunnett's multiple comparison test)

**V_{max} value significantly different ($P < 0.01$) than for HEK-WT-MRP1 (one way ANOVA, Dunnett's multiple comparison test)

Molecular Pharmacology Fast Forward. Published on June 13, 2016 as DOI: 10.1124/mol.116.103648
This article has not been copyedited and formatted. The final version may differ from this version.

Figure 1

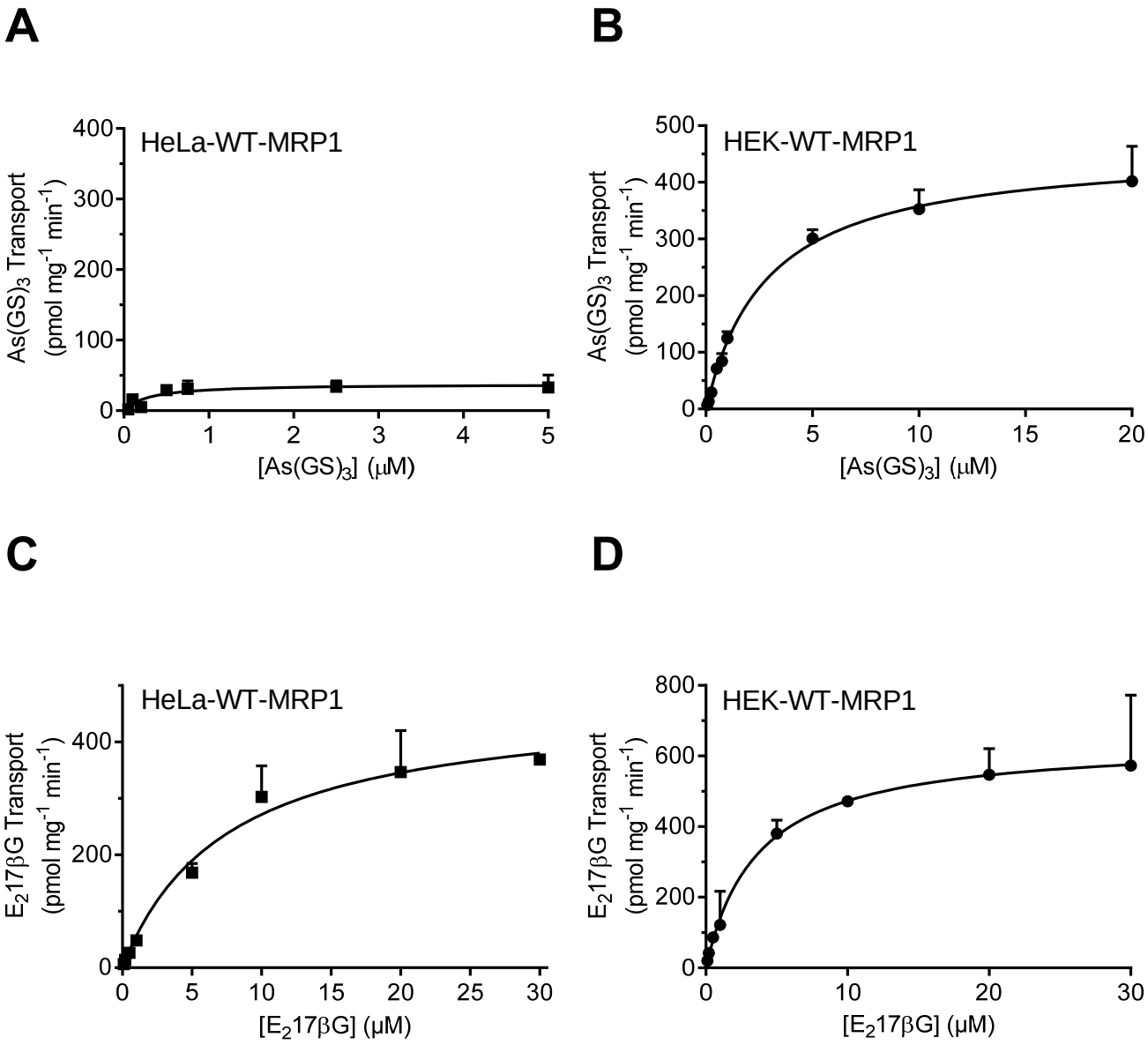

Figure 2

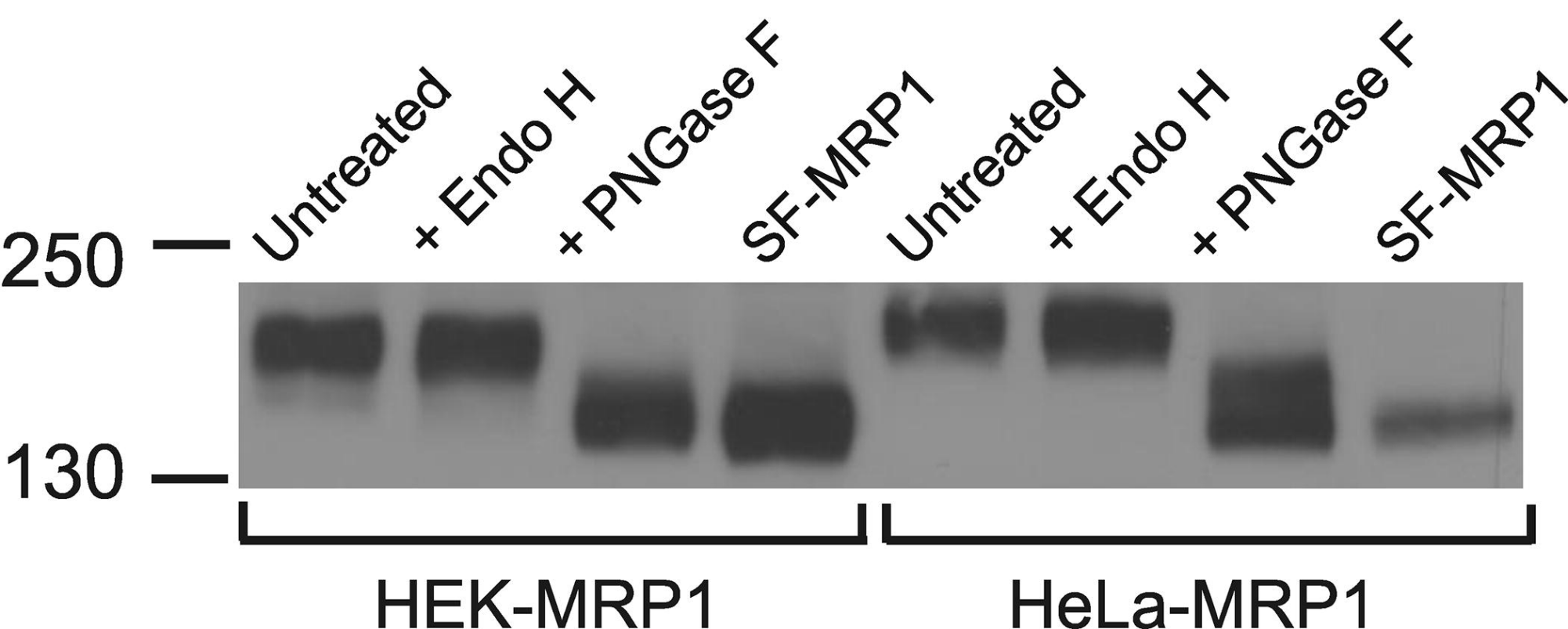
Untreated
+ Endo H
+ PNGase F
SF-MRP1
Untreated
+ Endo H
+ PNGase F
SF-MRP1
250
130
HEK-MRP1
HeLa-MRP1

Molecular Pharmacology Fast Forward. Published on June 13, 2016 as DOI: 10.1124/mol.116.103648
This article has not been copyedited and formatted. The final version may differ from this version.

Figure 3

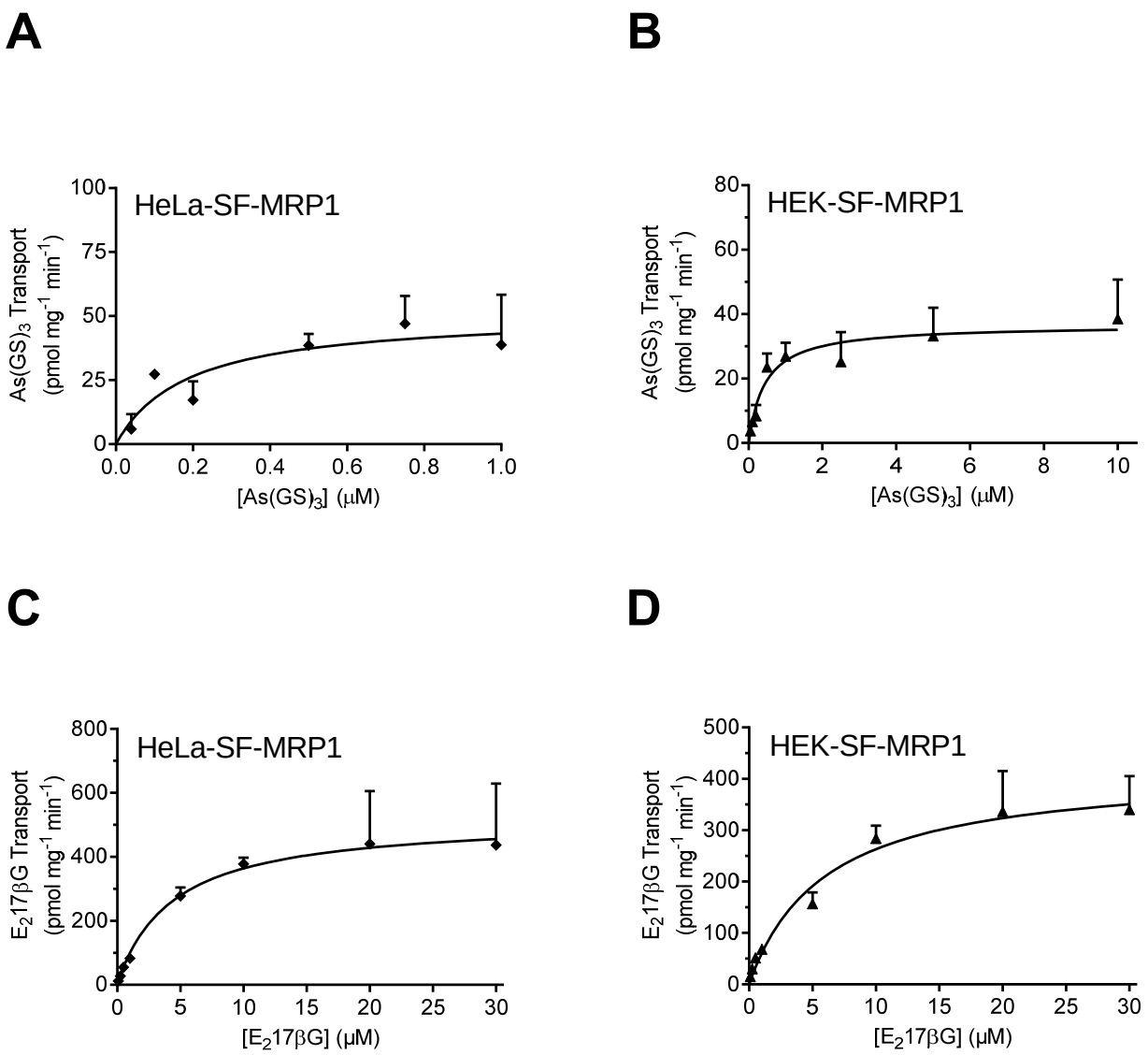

Molecular Pharmacology Fast Forward. Published on June 13, 2016 as DOI: 10.1124/mol.116.103648
This article has not been copyedited and formatted. The final version may differ from this version.

Figure 4

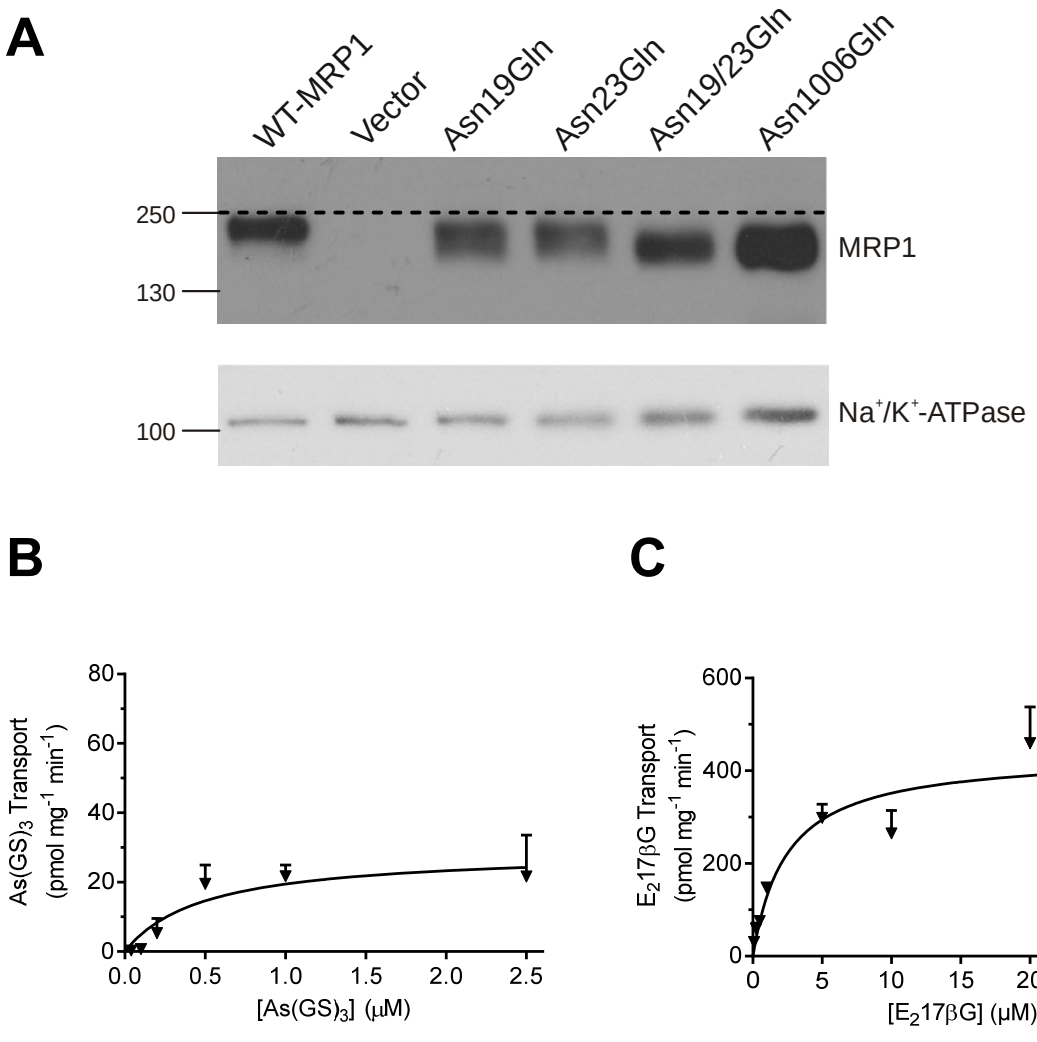

Molecular Pharmacology Fast Forward. Published on June 13, 2016 as DOI: 10.1124/mol.116.103648
This article has not been copyedited and formatted. The final version may differ from this version.

Figure 5

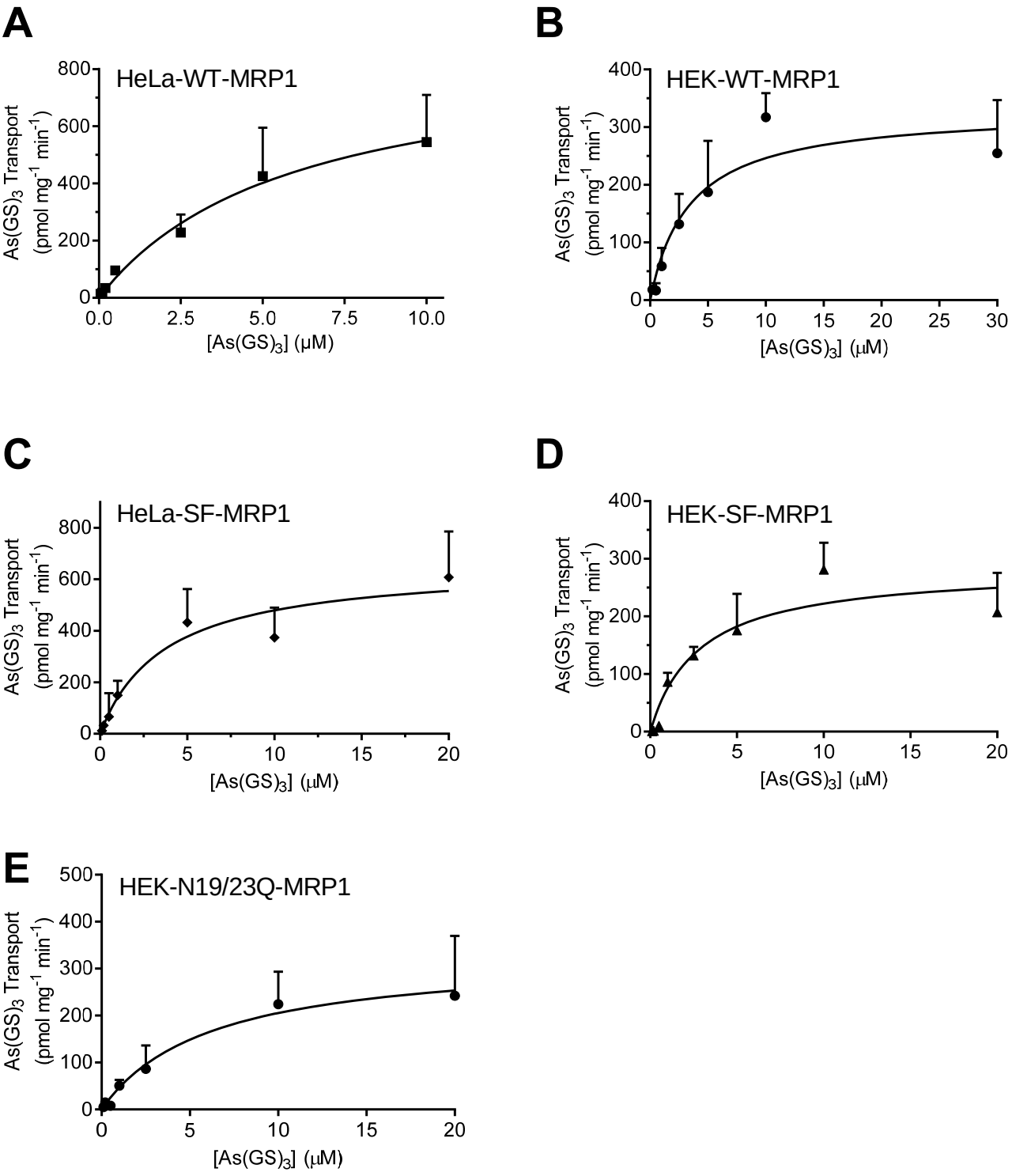

Molecular Pharmacology Fast Forward. Published on June 13, 2016 as DOI: 10.1124/mol.116.103648
This article has not been copyedited and formatted. The final version may differ from this version.

Figure 6

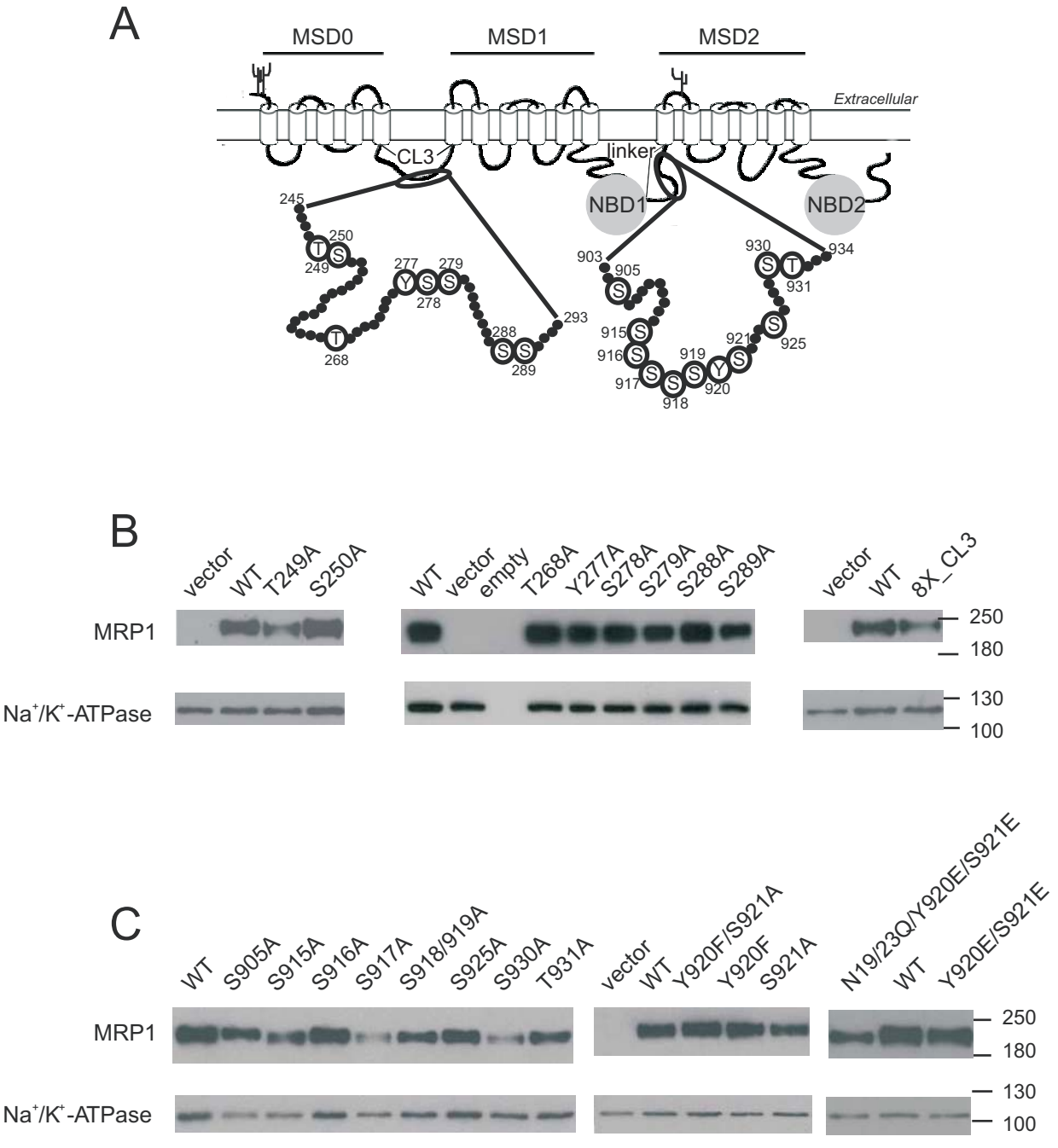

Molecular Pharmacology Fast Forward. Published on June 13, 2016 as DOI: 10.1124/mol.116.103648
This article has not been copyedited and formatted. The final version may differ from this version.

Figure 7